CHALMERS
UNIVERSITY OF TECHNOLOGY

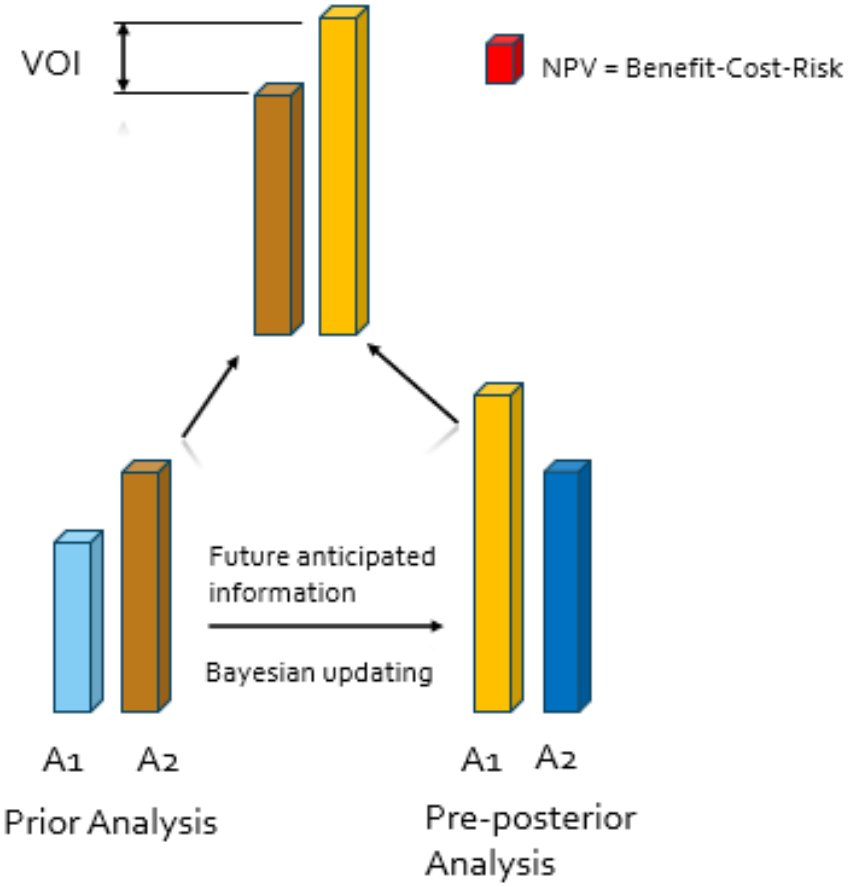

The value of hydrogeological information in tunnel design in rock

Evaluating VOIA to support pre-investigation decisions

Master's thesis in Infrastructure and Environmental Engineering

Rajesh Ulak

DEPARTMENT OF ARCHITECTURE AND CIVIL ENGINEERING
DIVISION OF GEOLOGY AND GEOTECHNICS

CHALMERS UNIVERSITY OF TECHNOLOGY
Master's thesis ACEX30
Gothenburg, Sweden 2025

MASTER'S THESIS ACEX30

The value of hydrogeological information in tunnel design in rock

Evaluating VOIA to support pre-investigation decisions

Master's Thesis in Infrastructure and Environmental Engineering

RAJESH ULAK

CHALMERS

Department of Architecture and Civil Engineering
Division of Geology and Geotechnics
CHALMERS UNIVERSITY OF TECHNOLOGY
Gothenburg, Sweden 2025

The value of hydrogeological information in tunnel design in rock
Evaluating VOIA to support pre-investigation decisions
Master's Thesis in Infrastructure and Environmental Engineering

RAJESH ULAK

Supervisor: Lars Rosén, Ezra Haaf and Sofie Axéen, Department of Architecture and Civil Engineering
Examiner: Lars Rosén, Department of Architecture and Civil Engineering

Master's Thesis 2025
Department of Architecture and Civil Engineering
Division of Geology and Geotechnics
Chalmers University of Technology
SE-412 96 Göteborg
Sweden
Telephone +46 31 772 1000

Cover:
The value of information is determined by comparing the optimal alternatives identified in the pre-posterior and prior analyses.
Department of Architecture and Civil Engineering
Göteborg, Sweden, 2025

The value of hydrogeological information in tunnel design in rock
Evaluating VOIA to support pre-investigation decisions

Master's thesis in Infrastructure and Environmental Engineering

RAJESH ULAK

Department of Architecture and Civil Engineering
Division of Geology and Geotechnics
Chalmers University of Technology

ABSTRACT

This thesis investigates the value of hydrogeological information in the design of infrastructure tunnels in fractured rock, with a focus on the *Kolmårdentunneln* project in Sweden. Uncertainty in hydraulic conductivity within fracture networks presents a major challenge in predicting groundwater inflow. To support design decisions under such uncertainty, this study applies a Value of Information Analysis (VOIA) framework integrated with hydrogeological modeling.

Two grouting alternatives, Alternative A1 (standard cement-based grouting) and Alternative A2 (cement with supplemental silica sol), were evaluated and compared against a no-grouting baseline (Alternative A0). Hydraulic conductivity for both general and Getå fractures was modeled using triangular probability distributions, and inflow simulations were performed using MODFLOW with multiple realizations. The analysis specifically examined tunnel sections prone to failure.

The VOIA was applied through a pre-posterior Bayesian framework, incorporating the reliability of hydraulic testing methods to estimate the benefit of future investigations. Cost-benefit analysis was used to determine whether additional data collection is economically justified. Although a positive expected value of information (127,861 SEK) was found, the optimal decision did not change from prior analysis, indicating that further investigation was not warranted under current conditions.

The results highlight the importance of incorporating uncertainty in tunnel inflow modeling and the potential of VOIA to support risk-informed and cost-effective design. Recommendations for future work include integrating spatial variability, improving computational efficiency, expert judgment for conditional probability, and combining VOIA with multi-option decision making.

Key words: Tunneling, Grouting, Modflow, Baysian analysis, Value of information

Acknowledgements

I would like to sincerely thank Professor Lars Rosén, my examiner and supervisor, for introducing the thesis topic and its underlying framework, and for his valuable guidance and support throughout the project. Special thanks to my supervisor Ezra Haaf, researcher at Chalmers University of Technology, for his helpful feedback and for coordinating with COWI to provide access to the groundwater model and data essential for this study.

I am especially grateful to Sofie Axéen, whose thoughtful feedback and active involvement helped shape the direction and quality of this thesis. Finally, I gratefully acknowledge COWI for supplying the model and data.

Rajesh Ulak, Gothenburg, August 2025

Contents

Notations

Abbreviation

CBA	Cost Benefit Analysis
DISV	DIScretization by Vertices
GUI	Graphical User Interface
NPV	Net Present Value(SEK)
PDF	Probability Density Function
PEST	Parameter ESTimation
SGU	Geological Survey of Sweden
SSR	Sum of Squares of Residual
VOIA	Value Of Information Analysis
WIC	Water Injection Capacity
WLM	Water Loss Measurement

Roman upper case letters

H	Depth below the groundwater table
K	Hydraulic Conductivity
K_{3d}	Mean of K based on Matheron's conjecture for 3D flow
K_{gr}	Hydraulic conductivity of grouted zone
P(F)	Probability of failure
P(D|F)	Probability of detecting failure given that failure exist
P(-D|F)	Probability of not detecting failure given that failure exist
P(D|-F)	Probability of false positive
P(-D|-F)	Probability of correctly identifying no failure

1 Introduction

1.1 Background

In underground construction projects, especially tunnel construction, the prognoses of geological conditions is always uncertain (Zetterlund et al., 2011). Likewise, assessing the inherent variability of hydrogeological factors is also a challenge (Merisalu et al., 2021). Hence, a thorough understanding of the subsurface conditions is essential for evaluating its characteristics before starting any tunneling project (Lindblom, 2010).

The prognoses are made based on field investigation, such as aerial imagery, seismic surveys, and core drilling, together with archival studies (Lindblom, 2010). However, gathering subsurface data is both costly and technically demanding. Furthermore, data retreived will always be specific to the exact location of sampling and hence, employing various methods becomes essential to make comprehensive interpretations between data points when characterizing rock or soil masses (Davis, 2002). To overcome these challenges, it is crucial to develop strategies for the design of investigation, ensuring both technical reliability and cost-effectiveness to optimize resource allocation in underground construction projects (Zetterlund et al., 2015).

In all stages of a project, uncertainty is present and must be considered (Merisalu et al., 2021). However, the degree of uncertainty is not constant; it is highest in the initial phase and gradually decreases toward the project completion as excavation advances and actual conditions inside and surroundings of the tunnel construction becomes available. But as the project advances, making design changes becomes increasingly difficult due to the significant time and money already invested, along with established infrastructure. Therefore, it is prudent to allocate optimal time and resources during the initial phase, where there is greater flexibility for modifications and adjustments. Early-phase planning and decision-making are critical for minimizing uncertainty and ensuring that the project can adapt effectively to emerging conditions .

In a tunnel project, engineering geologists primarily encounter two types of challenges: stability issues and water inflow (Zetterlund et al., 2011). In Sweden, water inflow problems are typically mitigated through conventional pre-excavation grouting in fans ahead of the advancing tunnel. While grouting is often time-consuming and costly, the expenses of not implementing it can be even greater. One of the key risks in this context is the lowering of the groundwater table, which can lead to subsidence in areas with compressible soils, the drying out of lakes, and difficulties for vegetation in accessing groundwater. Potential preventive measures include enhancing the tunnel's sealing and implementing artificial groundwater recharge (Sundell et al., 2019).

Effective tunnel grouting is achieved when the design is tailored to the specific geological conditions of the site (Gustafson and Walke, 2012). To estimate flow conditions around the tunnel, it is essential to characterize the water-bearing fracture system. In tunneling projects, limits are often set on the allowable inflow into the tunnel as a whole or for specific sections (Merisalu et al., 2020). The maximum permissible inflow is typically expressed as a volume per unit of time and tunnel section, with separate requirements for the construction and operational phases .

The key parameters used to describe the hydrogeological properties of the rock mass are hydraulic conductivity and transmissivity, which can vary significantly over short

distances (Gustafson and Walke, 2012). Therefore, estimating the order of magnitude of hydraulic conductivity is necessary for a representative assessment of groundwater flow through the rock mass. A hydrogeological simulation model is employed to predict the expected behavior of the system, considering uncertainties in parameters such as the hydraulic conductivity of the deformation zone before and after grouting (Freeze et al., 1992).

Extensive research has been conducted over the past few decades to develop advanced analytical solutions for estimating water inflow into tunnels, with many solutions focusing on calculating the discharge rate per unit tunnel length for practical applications (Xia et al., 2018). These analytical approaches have been further enhanced through the use of commercial software such as ABAQUS and COMSOL, which have been employed to create cross-sectional and steady-state models for simulating tunnel discharge. Additionally, 3D numerical models have been employed to simulate groundwater flow into tunnels. For example, MODFLOW and FEMWATER to assess the hydrogeological impacts of tunnel excavation. Similarly, FLAC3D to analyze pore pressure distribution around tunnels.

As stated by Freeze et al. (1992), data are valuable only when they assist in making decisions between different courses of action. It is acknowledged that every decision alternative carries a probability of failing to meet its performance objectives. This probability of failure represents the risk associated with each alternative. Risk reflects the uncertainty in the design parameters, and this uncertainty can be reduced through data collection. The worth of data is evaluated by comparing the cost of data collection to the expected value of the risk reduction it offers.

Value of information analysis (VOIA) is one such method used to assess the benefit of further investigation (Bedford & Cooke, 2001), similar to data worth analysis introduced by Freeze et al. (1992). VOIA supports decision-making by helping determine the appropriate scope and extent of investigations (Zetterlund et al., 2015). The core idea is to balance the cost of acquiring new information against the potential benefits of reducing uncertainty and minimizing the risk of making suboptimal decisions. Based on Bayesian statistics and traditional cost-benefit analysis, VOIA estimates the expected economic value of performing an investigation before it is conducted. The process of calculating the expected value of information is visually illustrated in Figure 1. The outcome of the analysis guides the selection of the most cost-effective investigation strategy by identifying which additional data would most significantly contribute to better-informed, lower-risk decisions.

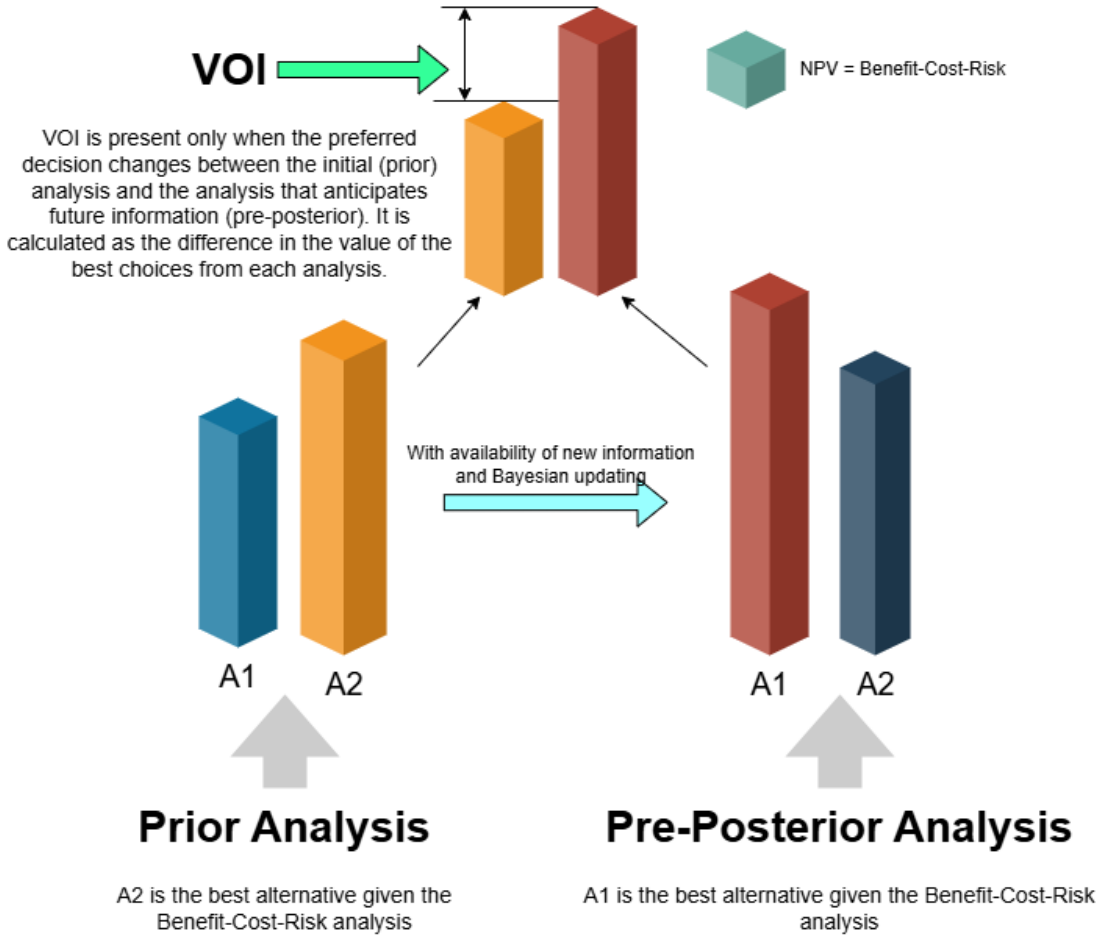

Figure 1: Graphical illustration of the VOIA.

Additionally, Zetterlund et al. (2015), emphasized the complexity of decision-making in tunnel construction and suggested that expert judgment could be used within VOIA to generate input data, offering an alternative to the reliance on complex models. Figure 2 presents an overview of the decision framework, incorporating the VOIA process. It follows an iterative cycle between analysis and field measurements.

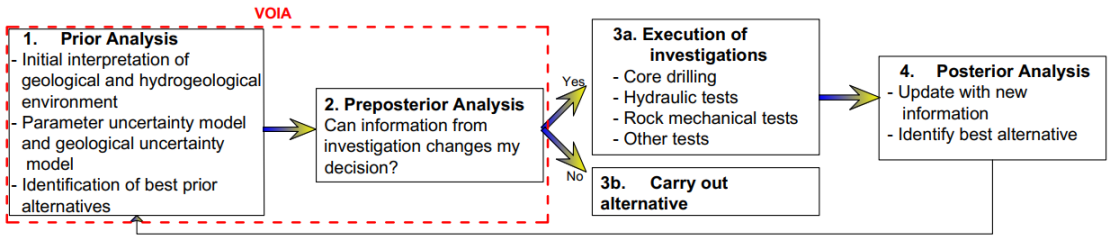

Figure 2: Overview of decision framework incorporating VOIA process. Modified from Zetterlund et al. (2015).

Given the complexity of underground construction, there is a need to further develop and apply VOIA in tunneling projects. This approach can enhance decision-making by systematically evaluating the impact of geological and hydrogeological uncertainties, ultimately leading to more effective risk management in underground construction.

1.2 Aim and obectives

1.2.1 Aim

This study aims to assess VOIA as a pre-investigation tool to aid decision-making on the scope of additional investigation programs. Hydraulic conductivity test data is utilized for pre-investigation and incorporated into the hydrogeological model to identify inleakage along the tunnel. VOIA is used to estimate the value of new information based on the reliability of the hydraulic testing program.

Two grouting design alternatives will be evaluated, differing in the number of grouting boreholes and the type of grouting material used. To achieve the study's aim, the following key questions need to be addressed:

1. Which grouting design is most suitable from both hydrogeological parameter data set and economic perspective?
2. Does new hydraulic test provide valuable information for decision-making?

1.2.2 Objectives

1. Analyze the geological and hydrogeological conditions influencing water inflow in tunnels.
2. Conduct simplified hydraulic modeling using prior information based on existing Cowi models (Trafikverket, 2022).
3. Define failure criteria based on leakage exceeding permit limit.
4. Assess the probability of failure using hydrogeological modeling results.
5. Estimate the economic impact of failure scenarios .
6. Compare alternative pre-excavation grouting designs through prior cost-benefit analysis (CBA).
7. Evaluate the reliability of hydraulic conductivity testing methods used in the study.
8. Assess the value of additional investigations by conducting pre-posterior analysis.
9. Provide final insights and recommendations for optimizing grouting design and risk mitigation in tunnel projects.

1.3 Limitations / Demarcations

1. Simplifications were made in the assignment and optimization of hydraulic conductivity. The spatial variability of hydraulic conductivity within geological objects and lithological units was not considered, with each unit instead being treated as a single, homogeneous entity.
2. The composition of the material filling the fractures is unknown, and variations in infill between different fractures may influence the prediction. Additionally, the variation along the depth and length is simplified.
3. To simplify the analysis, the fracture orientation was assumed completely vertical without accounting for its dip.

4. Flow observations (e.g., discharge rates) were not used for manual calibration, potentially affecting parameter reliability due to dependence on head data alone.
5. The graphical user interface (GUI) ModelMuse, utilized in this study, presents certain limitations, particularly in its user-friendliness, difficulty in troubleshooting errors, and relatively long runtime during model run.
6. The potential deterioration of sealing properties over time is not accounted for this study.
7. The variation in hydraulic head was not taken into account. As the model operates under steady-state conditions, fluctuations in water levels and their influence on inflow were not considered.

2 Case study

This chapter introduces the tunneling projects examined in this study. The tunnel selected for analysis, *Kolmårdentunneln* is part of the *Ostlänken* project. The *Ostlänken* is a planned high speed railway in Sweden, designed to connect Södertälje (just south of Stockholm) to Linköping (Trafikverket, n.d.). The *Ostlänken* is a planned double track railway spanning approximately 160 km between järna and Linköping and planned to increase train capacity and supports the expansion of labor market regions, facilitating smoother commuting and promoting regional development. Construction is underway for certain sections, while others are still in the planning phase. The *Ostlänken* is scheduled to open for traffic in 2035.

Figure 3: Map illustrating the route of *Ostlänken* from Järna to Linköping, highlighting the position of *Kolmårdentunneln* along with its geographic location. Modified from Trafikverket (n.d.).

2.1 Study area

Kolmårdstunneln is an 8-kilometer-long tunnel segment of the *Ostlänken* project (Trafikverket, 2024).The tunnel is located beneath the Kolmården forest, an area of considerable ecological, cultural, and recreational importance. The landscape features rolling terrain with ridges, valleys, and small lakes. The region is rocky, with morainic deposits and bedrock exposed near the surface in several spots. A notable feature is Getåravinen, a striking ravine that bisects the forest, creating a natural divide. Within this ravine is Getåbacken, a stream with high natural value, flowing through wetland forest and emptying into Bråviken.

Near the southern end of the tunnel lies lake Skiren, a deep lake with high ecological

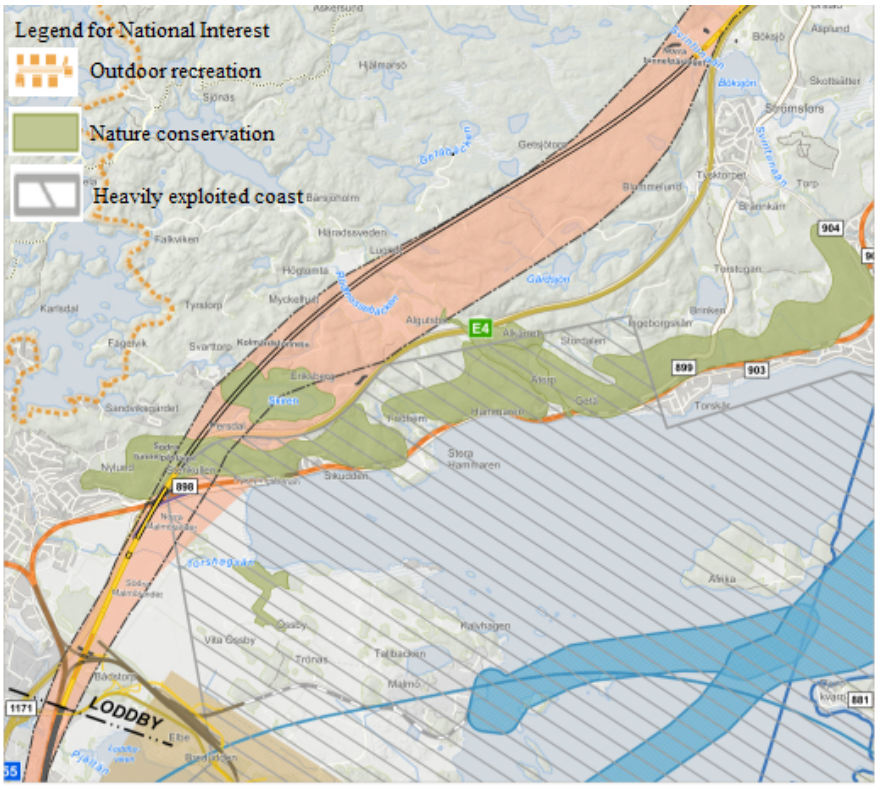

Figure 4: Figure showing national interest in study area (Trafikverket, 2024)

.

value Trafikverket (2024). It is designated as a "riksintresse" (national interest) for nature conservation, owing to its unique glacial relic species and clear waters, as shown in Figure 4, along with other areas of national interest. Additionally, part of the study area falls within the Natura 2000 network, which safeguards habitats and species of European importance. The Algutsbo Natura 2000 site, located near the tunnel alignment, includes wetlands and forests rich in biodiversity.

2.2 Geologic conditions

The study area is underlain by precambrian crystalline bedrock, primarily composed of granite and gneiss, with an isolated parts of amphibolite (Trafikverket, 2024). In the higher terrain, the soil profile typically comprises till resting on bedrock, with localized depressions containing deep accumulations of organic soils or sediments. Much of the elevated landscape features exposed bedrock at the surface. In contrast, the low-lying areas surrounding lakes Gullvagnen, Strålen, and Böksjön are characterized by deposits of wave-washed postglacial sand and silt. In the Getå ravine, the valley is composed of coarse-grained friction material resting on a water-bearing bedrock layer. This friction soil is covered by a silt-rich layer, with the thickness of these fine sediments varying throughout the valley. In some areas, the total soil depth surpasses 30 meters. The map depicting bedrock in the study area, as interpreted by SGU, is shown in Figure 5 whereas the soil type across the area is depicted in Figure 6.

In the northeastern part of the *Kolmårdstunneln* alignment, the bedrock is mainly composed of older gneissic granite, which transitions into younger coarse porphyritic granite with eye-gneiss (Trafikverket, 2022). Moving towards the middle of the tunnel

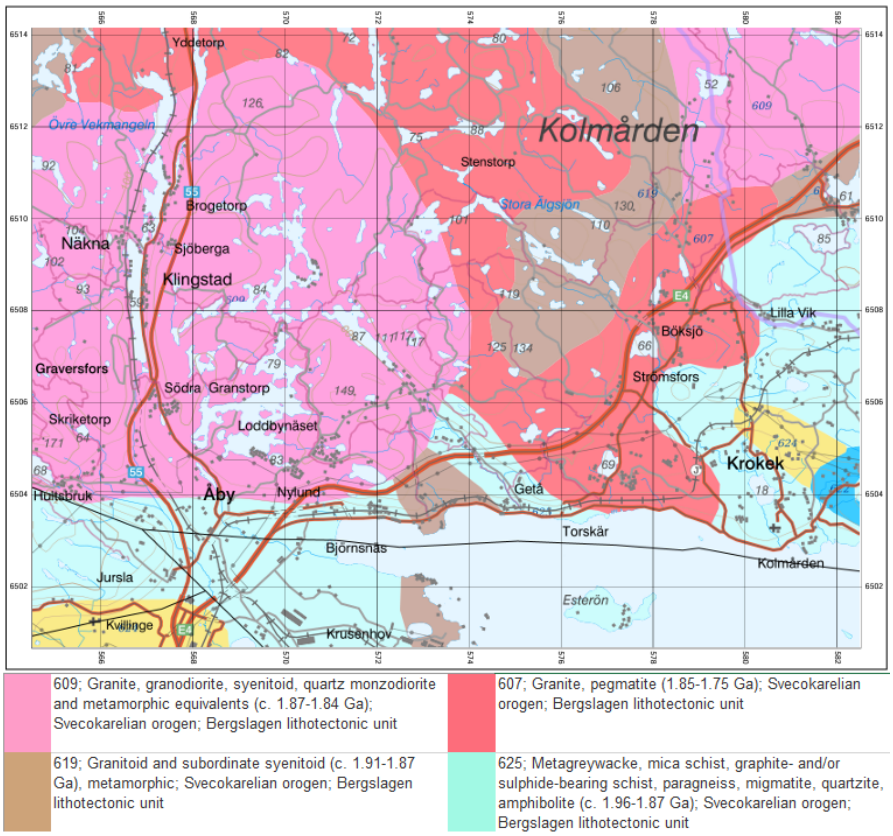

Figure 5: Map illustrating bedrock in study area as interpreted by SGU (Sveriges geologiska undersökning, 2021a).

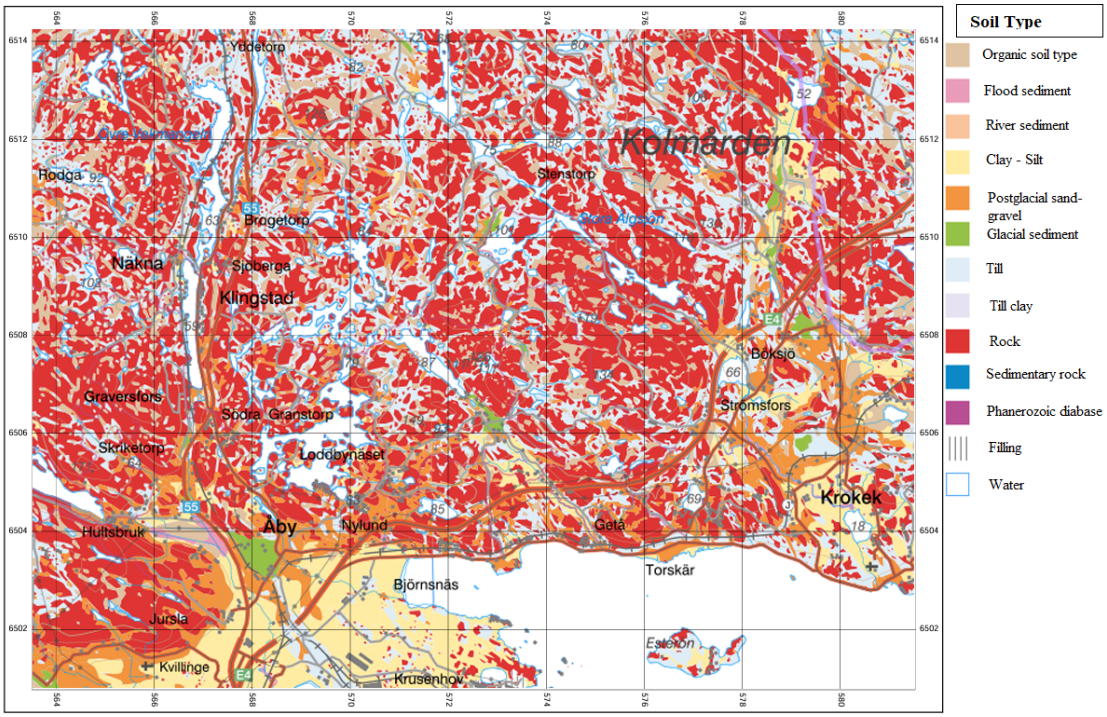

Figure 6: Map showing the soil type in study area interpreted by SGU (Sveriges geologiska undersökning, 2021b).

section, the bedrock consists of older metamorphosed sedimentary rocks, while in the southwestern section, the bedrock shifts to predominantly younger coarse porphyritic granite.

The region is shaped by the Bråviken Fault Zone, a major tectonic feature that has created steep slopes, fractured rock, and complex groundwater flow patterns, particularly in areas like Getåravinen (Trafikverket, 2024). Groundwater conditions vary, with shallow flow occurring in porous sediments and deeper, pressurized flow in fractured bedrock, potentially leading to artesian conditions. These geological characteristics present significant challenges for construction, including issues with stability, water inflow to tunnel constructions and overall a need for careful management of groundwater. A detailed map illustrating the deformation zone in the area, as interpreted by SGU, is displayed in Appendices A.1 and A.2 .

2.3 Hydrogeological conditions

The hydrogeological conditions along the Stavsjö–Loddby section are closely linked to the geological variability of the area (Trafikverket, 2024). Groundwater flow primarily occurs within the friction soil and the fractured bedrock . In elevated and hilly areas, unconfined groundwater aquifers are present, where infiltration is largely driven by precipitation due to the permeable nature of the till. These open aquifers allow relatively direct recharge and flow paths, especially in areas lacking low-permeability cover layers such as clay or peat. In contrast, in zones where clay or peat is present, particularly in depressions and wetland areas, semi-confined or confined aquifers can develop, restricting vertical groundwater movement and potentially generating localized artesian conditions.

South of the Bråviken escarpment, in the former glacial marine environment, the fine-grained sediments (glacial and postglacial clays and silts) significantly reduce vertical permeability (Trafikverket, 2024). Here, deeper groundwater flow is mainly concentrated in the underlying friction soils, which serve as important aquifers. In these layers, artesian pressures have been observed, indicating upward hydraulic gradients and suggesting that groundwater recharge may occur from adjacent higher elevation areas where till or bedrock outcrops are present.

In the Stavsjö-Loddby section, Trafikverket conducted hydraulic tests, including falling head and slug tests, at 51 sites, with the results from 41 locations being analyzed (Trafikverket, 2022). The purpose is to assess the local permeability of the soil around the test pipe. The calculated hydraulic conductivity varied between 3.8E-8 m/s and 2.9E-3 m/s. Additionally, a test pumping was performed at one site, yielding a hydraulic conductivity of 5.5E-7 m/s. Water loss measurements, carried out in core boreholes at 20 sites, indicated a hydraulic conductivity range of 3.9 E-8 m/s to 1.9E-6 m/s. The detailed results are provided in Appendices B.1, B.2 and B.3.

To assess the hudraulic conductivity in rock, data from water loss measurements and information from SGU's well data have been used. Based on the SGU map, the hydraulic conductivity in the area ranges approximately from 1E-8.5 to 1E-6 m/s. In comparison, values derived from water loss measurements conducted in core and percussion drill holes fall within the range of 9.09E-10 to 2.85E-7 m/s. The summary of bedrock conductivity is provided in appendix B.4 while the spatial distribution of hydraulic conductivity values obtained from the SGU data is presented in Figure 7.

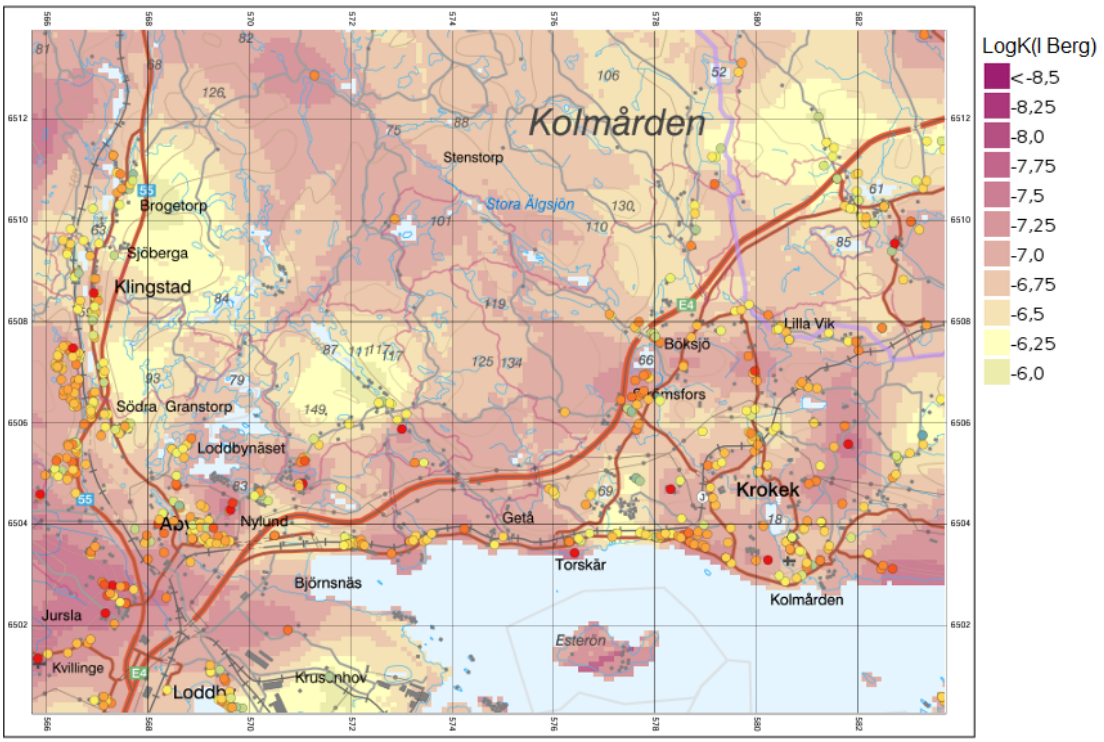

Figure 7: The Hydraulic conductivity around the study zone as interpreted by SGU (Sveriges geologiska undersökning, 2023).

2.4 Tunnel structure

Kolmårdstunneln is designed as a double-track rock tunnel, allowing high speed rail operation while ensuring structural stability (Trafikverket, 2024). The main tunnel features an open cross sectional area of 91 square meters, designed to reduce pressure buildup caused by trains travelling at high speeds (Trafikverket, 2021). To facilitate maintenance and emergency service, a parallel service tunnel runs approximately 7 km alongside the main tunnel (Trafikverket, 2024). Cross tunnels are strategically placed every 400 meters to create interconnections between the two . The service tunnel has an open cross-sectional area of 31 square meters, which is expanded near the connection points to accommodate emergency vehicle groupings (Trafikverket, 2021). The two tunnels are positioned 15.5 meters apart, but this distance is reduced to 10 meters at the widened sections to enhance functionality and safety. Additionally, four separate access tunnels at Böksjö, Svartgölen, Rödmossedn, and Persdal to facilitate excavation and logistical support during construction (Trafikverket, 2024). The first access tunnel runs parallel to the main railway tunnel, approximately 250 meters northward, connecting at km 95+200. The second access tunnel extends southward from km 97+600 and exits at Lake Svartgölen, about 800 meters southeast of km 97+300. The third access tunnel connects at km 100+000 and follows a circular path, emerging at the surface approximately 150 meters south of km 99+800. The final access tunnel connects at km 102+000 and curves northward, reaching the surface directly above the connection point of the main railway tunnel. The typical cross-section of the railway tunnel, the layout of the main and service tunnels, and the tunnel profile, including depth variations from the ground surface at the tunnel closure to a maximum of 142 meters before Getåravinen, are all illustrated in Figure 8 .

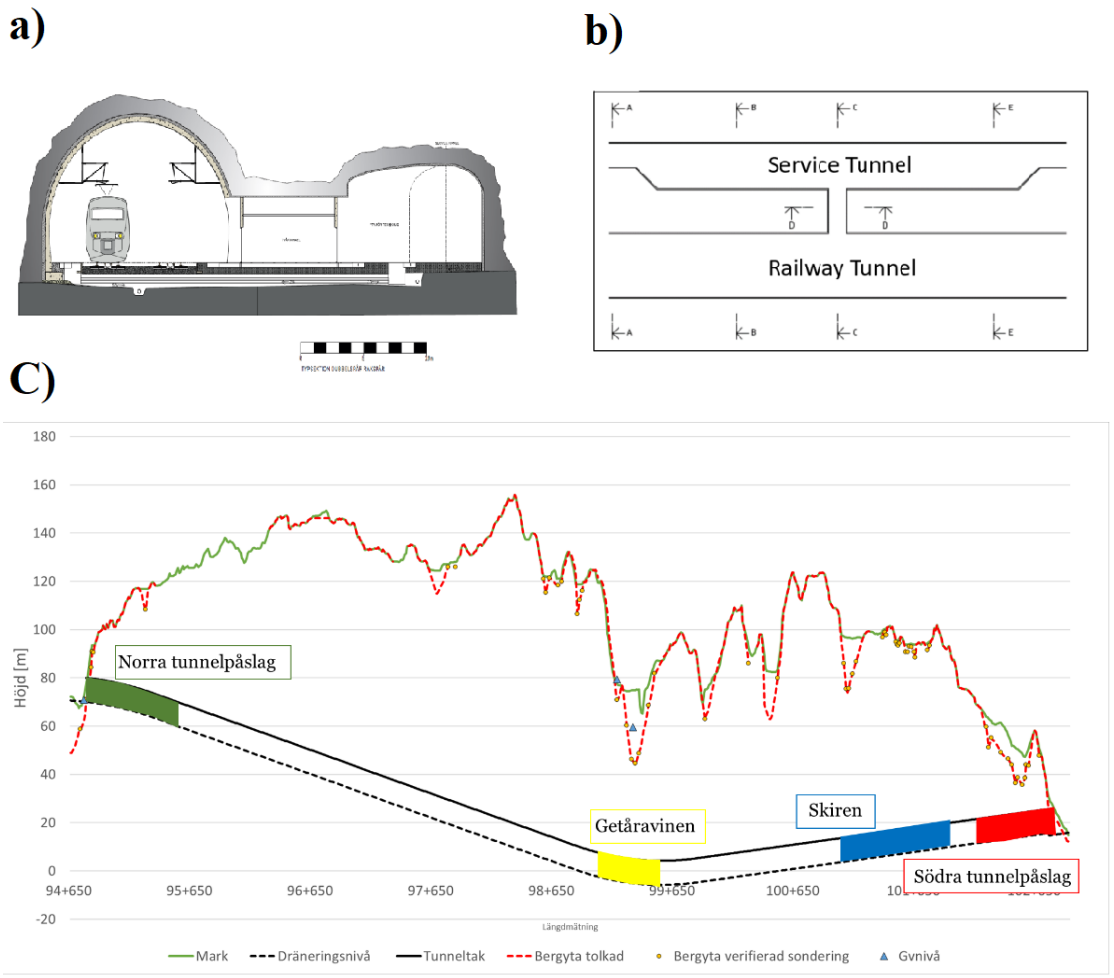

Figure 8: (a) Typical cross-section of the railway tunnel (Trafikverket, 2024). (b) Plan view showing the main and service tunnels (Trafikverket, 2021). (c) Tunnel profile with depth variations, reaching a maximum of 142 meters before Getåravinen (Trafikverket, 2022).

2.5 Grouting design

During tunnel construction in rock masses, cracks and deformation zones are critical factors, as they influence hydraulic conductivity and the connectivity of fractures. These features create pathways that facilitate the movement of significant volumes of water, posing challenges to the construction process. Systematic pre-grouting is commonly applied to minimize the water ingress into tunnels. The technique involves injecting grout into rock fractures to establish a low-permability barrier around the tunnel (Gustafson et al., 2004). To achieve this, a series of grouting boreholes are drilled around the tunnel perimeter and angled forward along the tunnel alignment (Gustafson et al., 2013). For effective grout penetration, these boreholes must be positioned to maximize the likelihood of intersecting fractures within the rockmass (Hernqvist et al., 2012). Grouting continued until the designated stop pressure is achieved (Hernqvist, 2009). Various grouting approaches, including the choice of grouting materials and design, are determined based on the fracture characteristics and the site's hydrogeological conditions (Grøv & Woldmo, 2012). As each grouting method involves different financial implications, acquiring detailed hydrogeological data and understanding site specific fracture

characteristics are crucial for selecting a cost-effecting strategies. Figure 9a shows a typical example of pre-grouting, highlighting how the grout spreads while 9b illustrate the grouting fan along with the arrangement of drilled holes.

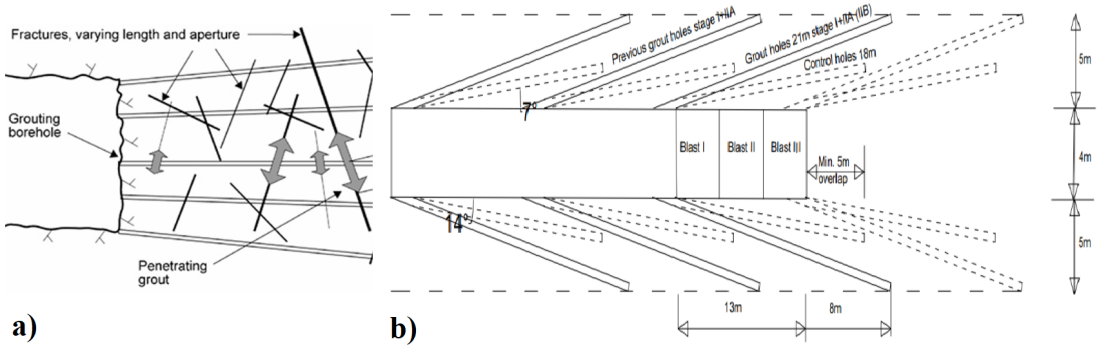

Figure 9: (a) Showing grout spreads from grouting hole into fractures of different sizes (Gustafson & Stille, 2005). (b) Showing the grouting fan along with the arrangement of the drilled hole (Grøv & Woldmo, 2012).

Control holes are mainly used to evaluate and monitor subsurface conditions, including measuring hydraulic conductivity following grouting. In contrast, grout holes are designed to inject grout into the ground to improve stability and reduce water penetration.

The final legal requirement set in the permit from the land and environmental court regarding water leakage limits had yet to be determined but provisional requirements were established for the injection design (Sweco, 2021). A leakage threshold of 15 liters per minute per 100 meters of tunnel was defined for most sections, whereas a stricter limit of 4 liters per minutes per 100 meters was imposed for the tunnel section near lake Skiren, an environmentally sensitive area. To comply with these varying constraints, different grouting classes are designed. The variations among these classes lie in the spacing of the holes, the pressure applied during grouting, and the type of grout used. The report Injection Concept Stavjö-Loddby by Sweco recommends a single cement injection for the low-risk section of the tunnel, whereas silica-based materials are suggested for injection in areas with stricter requirements (Sweco, 2021).

3 Methods

The methodology in this study is divided into two parts to provide both a conceptual overview and a detailed technical account. The first part outlines the general framework and is presented in Section 3.1, while the second part focuses on the specific methods and techniques applied at each stage, as detailed in Sections 3.2 and 3.3.

3.1 General overview

The methodology adopted in this project comprises two main components: (1) hydrogeological simulation model and (2) Value of Information Analysis (VOIA). The groundwater model, provided by COWI, was used to evaluate the impact of parameter uncertainty on the performance of grouting designs. All simulations were carried out using ModelMuse.

A process flowchart outlining the major steps of the project is presented in Figure 10, organized into two distinct sections: hydrogeological simulation model and value of information analysis. The tasks are arranged in chronological order, with all activities related to hydrogeological simulation model completed prior to initiating the VOIA phase. A brief description of each task is provided below for further clarification.

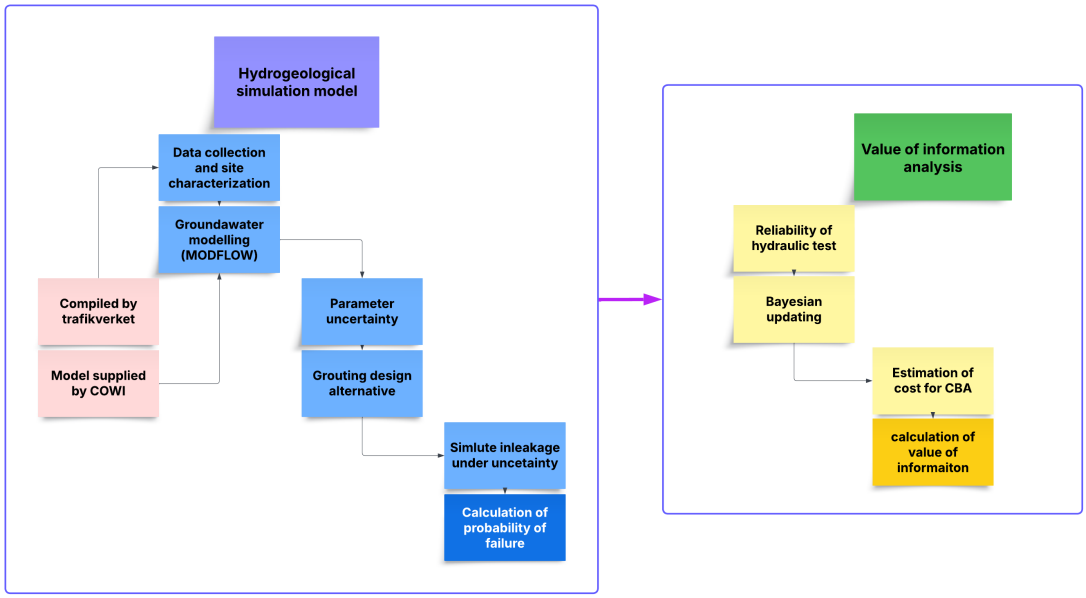

Figure 10: Overview of the methodological workflow.

3.1.1 Data collection and site characterization

An initial understanding of the hydrogeological conditions was developed using falling head tests, pump tests, and borehole water loss measurements. The data for these tests were supplied by Trafikverket.

3.1.2 Groundwater model

A steady-state groundwater model, provided by COWI, was developed using MODFLOW within ModelMuse. The model incorporates geological layering, hydraulic

boundaries (e.g., constant head conditions for lakes), and recharge settings. It simulates groundwater heads and tunnel inflows under varying hydrogeological scenarios.

3.1.3 Parameter uncertainty

Hydraulic conductivity of fracture zones is treated as uncertain and represented by triangular probability distributions. Here, the triangular distribution reflects the uncertainty in the overall hydraulic conductivity value of each fracture zone, rather than spatial variability along the fracture itself. Sampling from these distributions is used to generate multiple realizations.

3.1.4 Grouting design alternative

Two pre-excavation grouting alternatives are modeled:

- Alternative A1: 20 boreholes with cement grout.
- Alternative A2: 30 boreholes, including 10 with silica sol grout, achieving a higher sealing factor.

3.1.5 Simulation of realizations

Multiple simulations were conducted to evaluate tunnel inflow for each grouting alternative across a broad spectrum of fracture hydraulic conductivities. This approach enables the identification of conductivity ranges associated with a higher likelihood of exceeding inflow thresholds, ultimately allowing the estimation of failure probability based on a triangular distribution of fracture properties.

3.1.6 Reliability of hydraulic testing

A key consideration in the methodology is the reliability of hydraulic testing methods used to characterize the subsurface conditions. In this study, the reliability is represented by an estimated probability of detecting failure if it exists, P(D|F), which plays a central role in the pre-posterior analysis within the VOIA framework. While this probability is not derived from site-specific calibration, it serves as a reasonable assumption to illustrate the method and assess its influence on decision-making outcomes.

3.1.7 Bayesian updating

Bayesian updating is employed in this study to revise the probability of failure based on anticipated investigation outcomes. By applying Bayes' theorem, prior beliefs, such as the probability of failure before further investigation, are updated using conditional probabilities linked to detection reliability. This process reflects how additional field information can reduce uncertainty and influence the selection of optimal grouting alternatives.

3.1.8 Estimation of cost for CBA

The total cost for each alternative includes the direct costs of pre-excavation grouting, estimated based on the number of boreholes, grouting fan length, and grout material used. For cases where the inflow requirement is not met, post-excavation grouting is assumed, and its cost is added as part of the failure cost. These cost estimates were derived from reference values reported in the literature by Zetterlund et al. (2011).

3.1.9 Calculation of value of information

The cost-benefit analysis is carried out through the following steps to determine the value of information.

- Prior analysis: Comparison of alternatives based on the expected Net Present Value (NPV) without incorporating additional data.
- Pre-posterior analysis: Assessment of the potential benefit of future investigations by incorporating detection probabilities and Bayesian updating.

Further investigation is recommended if the pre-posterior analysis suggests a change in the optimal decision and results in a higher net present value (NPV) compared to the prior analysis. The value of information is quantified as the difference in NPV between the optimal alternatives identified in the pre-posterior and prior analyses.

3.1.10 Sensitivity and risk evaluation

Sensitivity analysis is performed by varying the reliability of hydrogeological tests to examine how detection probability affects decision-making, VOI, and failure risk. A second sensitivity analysis is conducted by varying the failure cost to observe how it impacts the outcomes of the VOIA.

3.2 Hydrogeological simulation model

Hydrogeological simulation model play a crucial role in understanding and managing groundwater systems (Moges et al., 2021). These models serve as powerful tools for predicting the behavior of aquifers under various conditions, thereby supporting informed decision making in underground construction. Key components of these models include detailed geological data, accurate representation of hydrogeological processes, and the application of advance numerical techniques. Despite their utility, hydrogeological models face challenges such as data availability, model complexity, and inherent uncertainties .

Due to the limited scope of field investigations, a significant portion of the data regarding soil depth and soil type has been obtained from external sources, primarily SGU's soil depth map. The interpreted soil layers at the surface are based on SGU's Quaternary geology map. To facilitate the numerical modeling process, the spatial distribution of soil types has been generalized, with increasing simplification toward the model's outer boundaries.

The hydraulic conductivity values for the soil and rock layers in the model have been determined based on field tests, expert knowledge, and reference literature (Trafikverket, 2022). The assigned values for different soil units are shown in Table 3.1.

Table 3.1: Hydraulic conductivity values for different soil units

Soil units	K_h (m/s)	K_v (m/s)
Clay	1×10^{-8}	1×10^{-8}
Sand	1×10^{-5}	1×10^{-5}
Till	5×10^{-7}	5×10^{-7}

Table 3.2 summarizes the hydraulic conductivity for the rock layer, along with the most likely values of fractured zones.

Table 3.2: Conductivity for bedrock and weak zone

Category	Condition	K_h (m/s)	K_v (m/s)	Remarks
Bedrock	Depth < 50 m	2.5×10^{-8}	2.5×10^{-8}	Mean of K based on Matheron's conjecture
	Depth > 50 m	2.9×10^{-9}	2.9×10^{-9}	
Weak zone	General fracture	2.00×10^{-7}	2.00×10^{-7}	
	Getå fracture	3.00×10^{-6}	3.00×10^{-6}	
	Getå weak zone	2.00×10^{-7}	2.00×10^{-7}	

The bedrock has been categorized into two conductivity zones based on depth from the rock surface (<50m, >50m). These zones characterize the overall rock mass and are derived from statistical analysis of all field tests conducted in the area. The hydraulic conductivity of the bedrock is represented by the mean value of K, derived in accordance with Matheron's conjecture and based on the evaluated hydraulic conductivity values within the bedrock. Hydraulic conductivity is adjusted at fractures and suspected weakness zones. The conductivity assigned to fractures represents a general value for weakness or crushed zones identified in multiple locations within the Kolmården area, based on water loss measurements in suspected zones.

The "Getå fractures" define the outer boundary of the Getå area, where the highest recorded hydraulic conductivity is observed. Situated between the two crushed zones labeled "Getå fractures" is the "Getå weak zone," which represents a rock region with significant water-conducting capacity. To simplify the model, the entire zone has been assigned a uniformly higher conductivity compared to the surrounding rock.

The groundwater recharge rate has been established at 200 mm/year across the entire area to prevent restrictions on infiltration, complemented by a drainage layer to handle excess surface water. This approach allows the conductivity of the uppermost layer to control groundwater recharge rather than being influenced by potential precipitation shortages.

Groundwater level data from active monitoring wells in the region have been utilized for model calibration. Figure 11a illustrates the locations of some of these wells, while Appendix C.1 provides details on the recorded water levels from all wells. Generally, the groundwater table in the area is near the surface, except in the Getå ravine, where it has been measured at approximately 13 meters below ground level in flatter sections. In this area, the groundwater table closely follows the ravine bottom. Most monitoring points are situated directly above or near the railway track, and groundwater levels in bedrock-drilled wells also typically remain close to the surface.

3.2.1 MODFLOW

The groundwater model was created and simulated using the MODFLOW6 numerical code within the Model Muse 5.3.1.0 graphical user interface . This version is the sixth

core release of MODFLOW and utilizes a generalized finite-difference method with control volume (Hughes et al., 2017). The code solves the flow equation for porous media in three dimensions. In contrast to earlier versions, this method enables cells to be hydraulically connected with all neighboring cells.

3.2.1.1 Model boundary and hydraulic boundaries

The model area is defined by a buffer zone extending approximately 3 kilometers from the planned tunnel. In regions where natural boundaries were difficult to identify at a relevant distance, the buffer zone was set to ensure no impact at the outer limits of the model. Large lakes in the region are considered positive hydraulic boundaries and are modeled using the "Constant head" (CHD) boundary condition.

A general drainage condition, "Drain" (DRN), is applied 0.5 meters below the ground surface to represent the surface runoff of precipitation into ditches, streams, and lakes. The hydraulic boundaries are depicted in Figure 11b. In the Getå ravine, the Getå stream is modeled as a drainage boundary condition (DRN) at the ravine's bottom. This condition is assigned to a presumed lower reservoir, as level measurements suggest the stream is in hydraulic contact with the friction soil. Lake Skiren is modeled as a drainage that follows the lake's bottom profile, with a pressure limit set at +84.4, which is considered the average water level of Skiren.

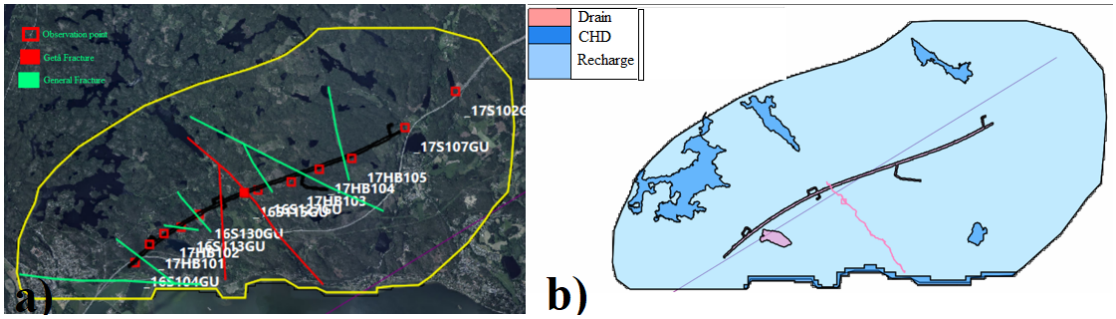

Figure 11: (a) Observation points in red square box and mapped fractures , Getå fracture in red and general fracture in green, in the study area. (b) Model domain showing the model boundary and applied hydraulic boundary conditions.

3.2.1.2 Model descritization

DISV(DIScretization by Vertices) grid option was used in the model which allows for an unstructured mesh composed of polygonal cells, providing flexibility in spatial resolution. The grid was refined around the tunnel and boundary conditions to capture detailed hydraulic gradients and flow patterns near these critical features. This localized refinement ensures that the influence of leakage inside the tunnel is more precisely represented without unnecessarily increasing the computational load across the entire model area.

Cells near the tunnel and access tunnels are 10 m x 10 m, those near lakes and fracture zones are 20 m x 20 m, and the rest of the model is represented by 40 m x 40 m cells, as illustrated in Figure 12a with a zoomed-in view of the rectangular area shown in the figure. The model area covers an area of approximately 67 km². Quadtrees refinement option in the modelmuse was used to achieve finer resolution in key areas of interest. The model includes 17 layers in the vertical direction, as shown in Figure 12b.

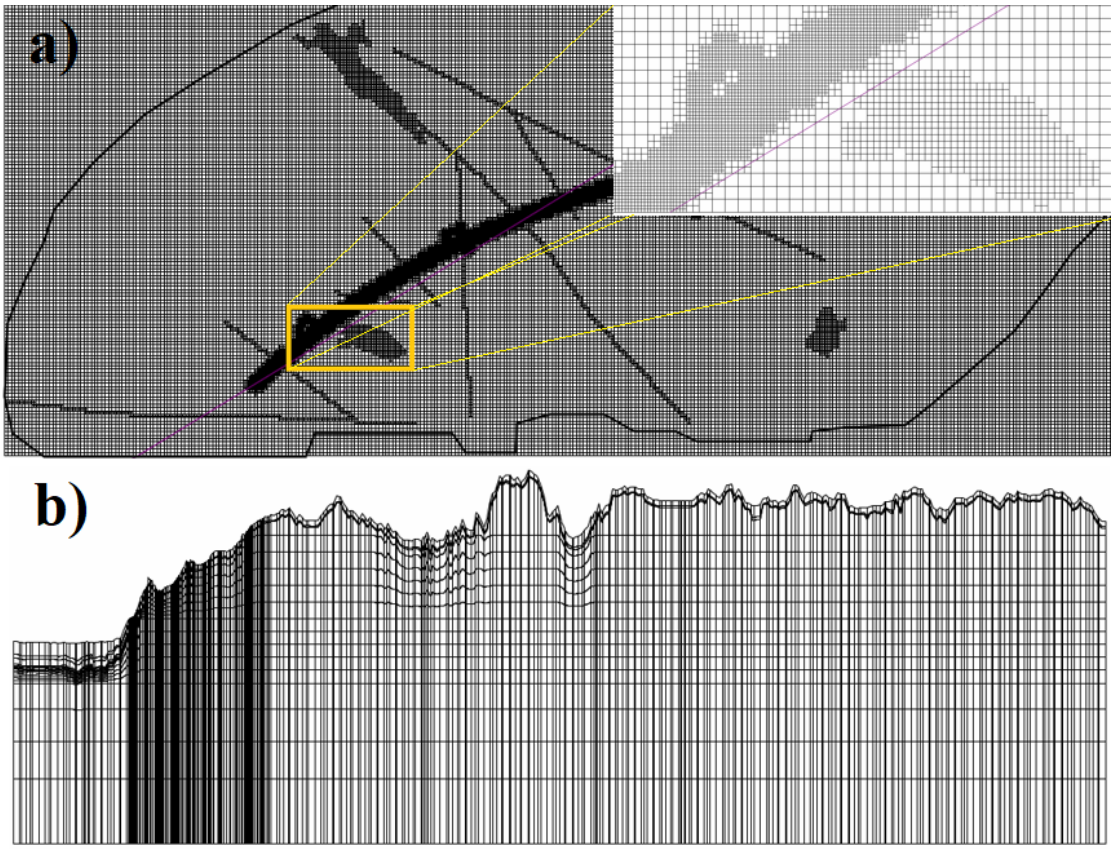

Figure 12: (a) Plan view of the model showing the cell matrix with a zoomed-in view of the rectangular area highlighted in the figure. (b) Section view illustrating layers in the model.

To address the numerical challenges associated with irregular cell geometries in the DISV grid, the Ghost Node Correction (GNC) package was employed (Panday et al., 2013). The GNC package enhances the accuracy of intercellular flow calculations by introducing virtual points, ghost nodes, that improve flow approximation across non-aligned cell interfaces. The explicit GNC option was selected to maintain numerical stability while still improving the fidelity of flow simulations across the unstructured mesh.

3.2.1.3 Object prioritization in ModelMuse

In ModelMuse, the assignment of spatially variable parameters and boundary conditions is managed through the use of objects, which can represent features such as geological units, fractures, or boundary conditions (Winston, 2009). When multiple objects overlap in space, the software applies them in the order they appear in the object list, from top to bottom, so that objects lower in the list take precedence and overwrite values assigned by those above them. This ordering determines which properties are ultimately assigned to each grid cell or finite element in the model. Therefore, careful management of object order is essential to ensure that model inputs reflect the intended conceptual model. For example, a river boundary condition should be placed above the underlying hydrogeological units to ensure its proper implementation, and smaller features such as fractures or sand lenses should be prioritized over more general materials if they occupy the same spatial domain. ModelMuse allows users to rearrange objects easily and

provides tools to visualize object influence, which aids in debugging and model refinement. A representative example is shown in Figure 13, where the grouting assigned to the general fracture has replaced the previously defined fracture in the overlapping area.

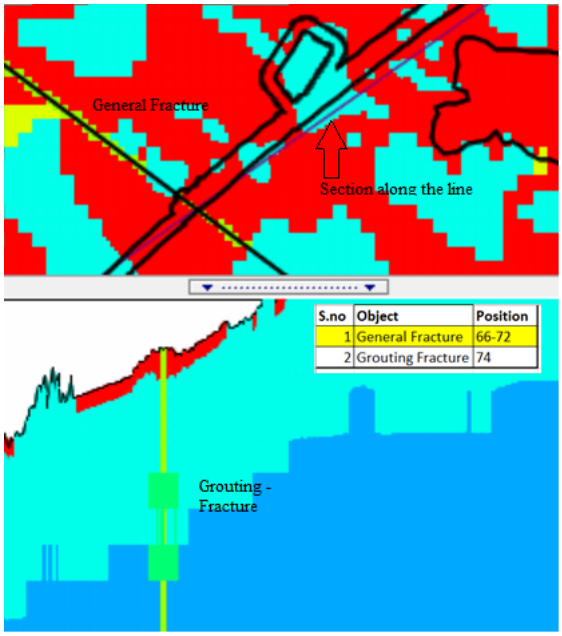

Figure 13: Showing priority of object.

3.2.1.4 Definition of head observations

Within ModelMuse, head observations are represented by point objects, which can be defined as either single-layer or multilayer, based on the characteristics of the observation well and its intersection with the model grid. Multilayer head observations are typically used when the observation well screens across multiple model layers. In this case, the observation object must include "Z formulas" that specify the vertical extent of the well screen, and the “Multilayer” checkbox in the “Calibration” tab must be selected. However, in this study, the “Multilayer” option was not selected. As a result, each head observation was treated as a single-cell observation, where ModelMuse automatically assigned the observation to the model cell with the longest length of intersection between the well screen and the model layers.

3.2.1.5 Sum of square of residual

To evaluate the model’s performance, the simulated hydraulic head is compared with observed values at each observation point. This comparison is quantified by calculating the sum of squared residuals, which represent the squared differences between simulated and observed heads. Squaring the residuals ensures that both overestimation and underestimation are treated equally, as it removes the effect of sign (i.e., negative or positive discrepancies). This approach not only neutralizes sign discrepancies but also emphasizes larger deviations, thereby providing a more sensitive measure of the model’s accuracy in replicating real-world conditions. A representative example of the computation for Realization 1 is included in Appendix D.2.

3.2.2 Parameter uncertainty

In hydrogeological modeling, parameters such as hydraulic conductivity often involve considerable uncertainty due to limitations in measurement, spatial heterogeneity, and insufficient data. In the Kolmården area, which is underlain by crystalline bedrock, groundwater movement through intergranular pores is minimal because of the rock's hardness and low permeability. Consequently, groundwater flow primarily occurs through fractures, whose complex geometry and limited accessibility make it difficult to determine their hydraulic properties. This study focuses on the uncertainty associated with these fractures. A common method for addressing this uncertainty is to represent uncertain parameters using probability distributions and to employ suitable sampling methods to carry the uncertainty through the model. One practical and frequently applied distribution for this purpose, where only limited information is available but most likely value and bounds are known, is the triangular distribution (Kissell and Poserina, 2017).

3.2.2.1 Triangular distribution

The triangular distribution is a type of continuous probability distribution defined by three parameters: the minimum value (a), the most likely value (c), and the maximum value (b) (Kissell and Poserina, 2017). Its shape forms a triangle, making it intuitive and straightforward to use, particularly in cases where data are scarce but expert judgment is available. Typical illustration of triangular distribution is presented in Figure 14

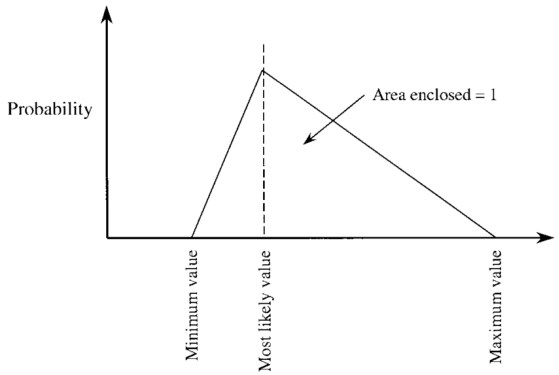

Figure 14: Illustration of typical triangular distribution (Murphy, 1999).

The probability density function (PDF) of a triangular distribution is defined as:

$$f(x) = \begin{cases} 0 & \text{for } x < a \\ \frac{2(x-a)}{(b-a)(c-a)} & \text{for } a \leq x \leq c \\ \frac{2(b-x)}{(b-a)(b-c)} & \text{for } c < x \leq b \\ 0 & \text{for } x > b \end{cases}$$

The triangular distribution applied to general fractures captures the uncertainty in the overall hydraulic conductivity of each fracture zone, rather than representing spatial variability along the fracture. For these fractures, hydraulic conductivity values range from 1×10^{-9} m/s at the lower bound to 1×10^{-6} m/s at the upper bound, with the most likely value (mode) at 2×10^{-7} m/s.

In contrast, the Getå fracture, a more permeable and geologically significant feature, was assigned a wider triangular distribution to reflect the uncertainty in the total hydraulic conductivity of this fracture zone. Its hydraulic conductivity spans from 1×10^{-9} m/s to 8×10^{-6} m/s, with a peak probability at 3×10^{-6} m/s, representing the higher expected transmissivity of this critical zone.

3.2.2.2 Sample selection

To capture the influence of uncertain parameters , hydraulic conductivity of general fractures and Getå fracture, on model outputs, sampling from the triangular distribution is critical. However, interval-based sampling from the triangular distribution may not adequately explore the distribution's tails, especially when the number of samples is limited. Therefore, a controlled sampling strategy was employed to ensure better coverage across the full range of the distribution, with increased emphasis on the edges (minimum and maximum), where extreme behavior can occur.

A nonlinear transformation technique was applied to the cumulative probability space. First, a linearly spaced uniform vector $u \in [0, 1]$ of size n was generated. To redistribute the sample density toward the edges, a power transformation was applied as:

$$u_{\text{modified}} = u^{1.5}$$

This transformation stretches values closer to 0 and 1 while compressing those near the center, effectively increasing the sampling density toward both distribution tails. To map the modified cumulative values to actual distribution values, a cosine-based transformation was then used:

$$x = a + (b - a) \cdot 0.5 \cdot (1 - \cos(\pi \cdot u_{\text{modified}}))$$

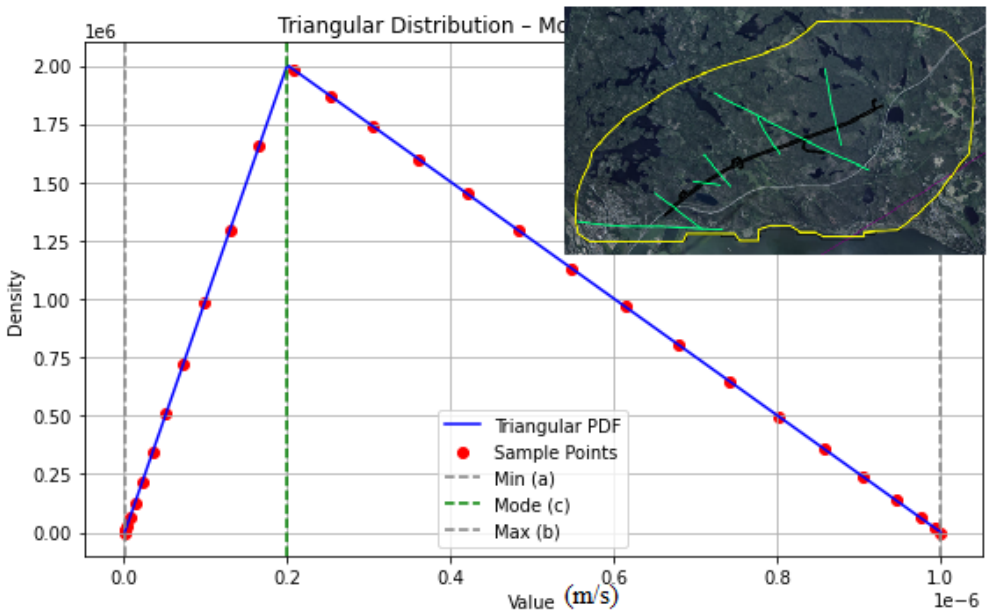

Figure 15: Triangle distribution for general fractures with more samples toward the edges

This formulation not only maintains the continuity and smoothness of the distribution but also ensures that edge values are better represented in the selected samples. This approach is particularly useful for uncertainty quantification, as extreme input values, though less likely, can lead to disproportionately large impacts on model outputs.

Figure 15 demonstrates non-uniform sampling, which concentrates more points near the lower and upper bounds to better capture the behavior at the distribution edges. Simlilarly, Figure 16 illustrate the selection of samples for getå fractures which have higher hydraulic conductivity than the general fractures.

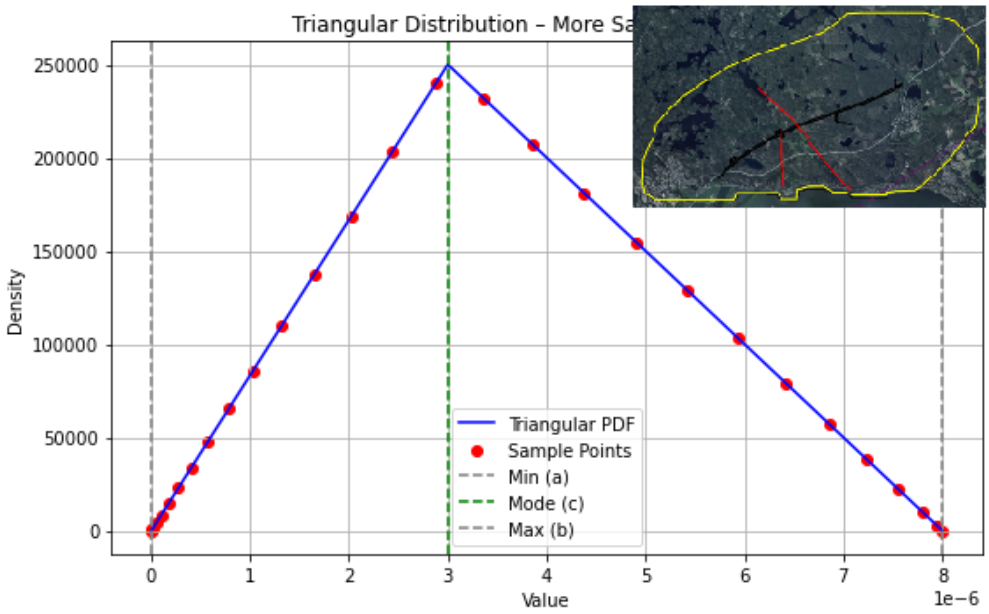

Figure 16: Triangle distribution for getå fractures with more samples toward the edges

The exponent in the power transformation (e.g., 1.5) can be tuned to control the degree of emphasis toward the tails. Larger values like 2.0 result in even more extreme edge bias, whereas values closer to 1.0 yield more balanced spacing. Conversely, using an exponent less than 1 (e.g., 0.5) would concentrate more samples near the center (most likely value).

This tailored sampling strategy strikes a balance between computational efficiency and distributional representation, making it well-suited for use in uncertainty modeling where the number of samples is constrained but edge behavior is critical. The selected value for hydraulic coductivity for different fracture is presented in Appendix D.1

3.2.3 Grouting designs

Two alternative grouting designs were developed to mitigate groundwater inflow into the tunnel and ensure adequate sealing, particularly in zones with higher hydraulic conductivity and fractured bedrock. These include sections intersecting identified fracture zones, where groundwater inflow is more likely. In this approach, a 10-meter-thick injection zone was applied in the model to represent the anticipated 6-meter practical injection zone, considering the grid discretization limitations around the tunnel. In Alternative Grouting Design 1, the hydraulic conductivity of the fractures was reduced to 1×10^{-7} m/s, corresponding to a sealing factor of 2. This reduction is based on the

most probable hydraulic conductivity value for general fractures. However, it is important to note that this assumption does not necessarily apply to all realizations, as fracture properties can vary significantly across different realizations. The same target hydraulic conductivity reduction was assumed for the Getå fracture and applied in the numerical modeling, ensuring consistency with the sealing performance criteria used for general fractures. After accounting for the 10 m model cell thickness, the adjusted hydraulic conductivity implemented in the numerical model was 1.67×10^{-7} m/s. Grouting design Alternative 1 consists of a standard setup featuring 20 boreholes per grouting fan, with cement-based grout used as the sealing material. This configuration represents a conventional approach, typically applied in conditions where moderate inflow control is sufficient and geological complexity is limited. The use of cement provides adequate sealing efficiency in most cases, though its performance may be less effective in fine or highly fractured zones. Figure 17 provides a visual representation of the grouting design for alternative 1.

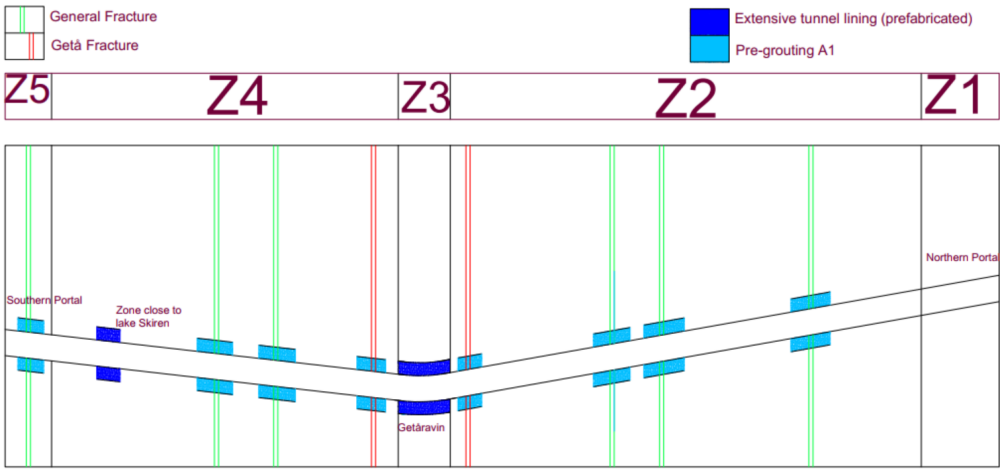

Figure 17: Illustrating the grouting design of alternative 1

For the identified weakness zones, namely the Getå ravine and the critical section beneath Lake Skiren (approximately 300 m in length), extensive sealing measures such as prefabricated sections were applied in both alternatives. As a result, these areas were excluded from the Value of Information Analysis (VOIA) to simplify the scope of this study.

Grouting Design Alternative 2 represents a more advanced and robust sealing strategy, aimed at achieving higher inflow control in challenging geological conditions. This alternative builds upon the standard configuration by incorporating an additional 10 boreholes per grouting fan, bringing the total to 30 boreholes, targeted at hydraulically sensitive or weak zones, exactly in the same location as in alternative 1. In addition to the standard cement-based grout used in the primary 20 boreholes, the supplementary 10 boreholes are injected with silica sol, a low-viscosity colloidal solution that enables deeper penetration into fine fractures and narrow apertures. This dual-material approach significantly enhances the sealing performance, achieving a sealing factor of 3, sealing hydraulic conductivity of 0.67×10^{-7} m/s, and after adjusting for cell thickness, the adjusted hydraulic conductivity implemented in the model was 1.11×10^{-7} m/s. The sealing factor is derived from the most probable hydraulic conductivity of the general fractures. However, as previously discussed, this assumed sealing factor does not hold

consistently across all realizations. The same target hydraulic conductivity was also applied to the Getå fractures.

Such a advanced design is especially effective in zones with high fracture density or where fine fissures limit the effectiveness of conventional grout materials. However, it also implies higher construction costs and material usage due to the greater extent of grouting. Both alternatives were assessed in terms of their effectiveness in reducing tunnel inflow and their implications for design feasibility.

The hydraulic conductivity values used in the model for each alternative are summarized in Table 3.3. These values were assigned to different geological zones based on known fracture locations, and areas where additional sealing measures were implemented. The table provides a clear comparison between the null case and the two proposed grouting strategies.

Table 3.3: Hydraulic Conductivity Values (in m/s) for Different Alternatives and Zones

Alternative	**General fracture**	**Getå fracture**	**Getå weak zone**	**Skiren sealing**
Null alternative	2.00E-07	3.00E-06	2.00E-07	2.90E-09
Alternative 1	1.67E-07	1.67E-07	1.67E-09	1.67E-09
Alternative 2	1.11E-07	1.11E-07	1.67E-09	1.67E-09

The probability of failure, P(F), for each alternative is estimated by comparing the modelled tunnel leakage with a predefined threshold that defines unacceptable leakage. To evaluate water inflow into the tunnel, a water balance analysis was conducted using the Zonebudget (ZONEBUD) program. This tool is capable of calculating the water budget for specific regions within the model, providing insights into the distribution and movement of water across the system.

3.3 Value of information analysis

3.3.1 Reliability of hydraulic test

This section discusses the hydraulic tests conducted to characterize the hydrogeological conditions of the Kolmården area.

3.3.1.1 Falling head method

A total of 51 falling head and slug tests were performed at various locations, but only 41 of them were considered for evaluation. The remaining 10 tests were excluded due to various issues, including non-functioning test pipes caused by blockages, unexplained rapid drawdown, dry conditions in the test pipe from the start, and human errors such as missing drilling logs. The testing methodology involved placing a pressure sensor in each well to monitor changes in pressure levels as the groundwater surface recovered to its original state. The results obtained from the falling head tests were subsequently analyzed using the AQTESOLV software to estimate key hydraulic properties of the subsurface. The other limitation of this method is that it provide only local estimate of permeability around the pipe's filter section. The typical illustration of the falling head method is shown in Figure 18.

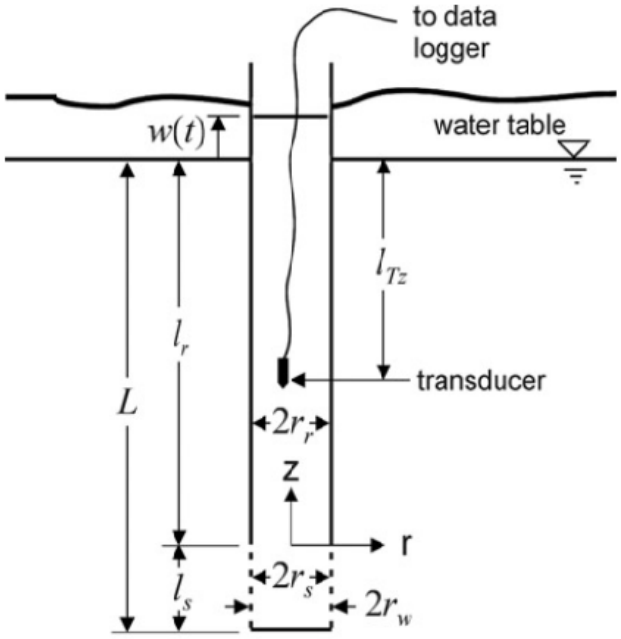

Figure 18: Typical illustration of slug test (Zurbuchen et al., 2002).

3.3.1.2 Pumping test

A pumping test was carried out at a single location, designated 17S122BR, over a two-week period to evaluate the hydraulic response of the surrounding aquifer. While the test provides useful insights, it does not adequately capture the natural variability of the aquifer, such as variations in permeability, stratification, or the presence of fractures. These heterogeneities can result in non-uniform responses that complicate data interpretation. Moreover, the positioning of the well screen (filter) significantly influences the outcome, as test results can vary depending on the alignment and depth of the filter within the aquifer. A typical illustartion of pumping test is presented in Figure 19

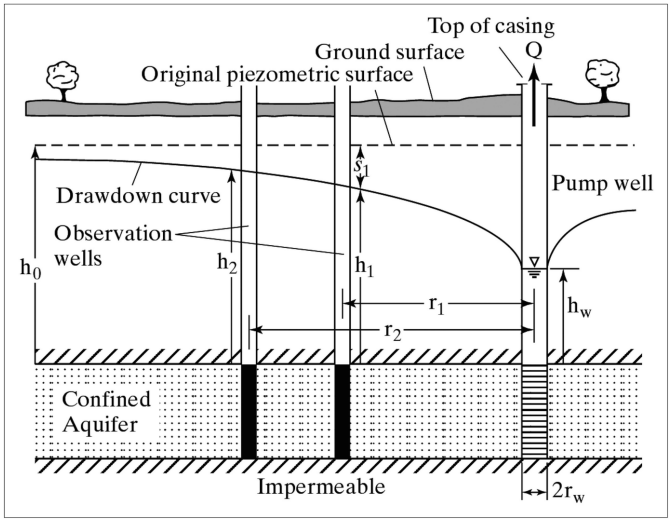

Figure 19: Typical illustration of pumping test (Sikdar, 2019).

3.3.1.3 Water loss measurement

Water loss measurements were conducted in boreholes at 20 different locations. Following the completion of core drilling, tests were performed using both single and double packers. The objective was to assess water loss across the entire or half-length of boreholes (using single packers) and within shorter intervals (using double packers) to obtain a more detailed understanding of permeability distribution. Two different measurement methods were applied, depending on the required level of accuracy. For higher precision, Water Injection Capacity (WIC) equipment was used, while in cases where lower accuracy was acceptable, a conventional water loss testing method was employed. A typical illustration of WLM is presented in Figure 20

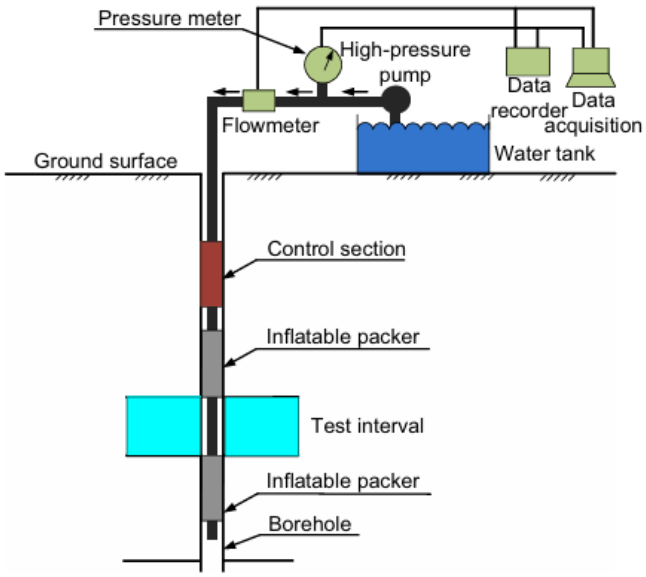

Figure 20: Typical illustration of WLM test (Chen et al., 2015).

WIC tests, which utilized both single and double packers, had a minimum detection limit of 2 ml/min, making them unsuitable for detecting flow in zones with very low

permeability, such as dense bedrock. The conventional method, with even higher detection limit, posed even greater risk of failing to register results in low permeability zones. As a result, both methods may underrepresent water loss in relatively impermeable sections, emphasizing the importance of selecting appropriate testing techniques based on the hydrogeological setting. There is also uncertainty related to the effectiveness of the packer system, which may result in leakage around the isolated test section. Additionally, fractures could be located outside the packered interval, potentially leading to missed flow zones and an incomplete assessment of the hydraulic properties.

3.3.1.4 Quality of investigation campaign

For the purpose of this thesis, a hypothesis was established stating that the methods used to characterize the hydrogeological properties carry a 20% probability of failing to detect critical features, such as fractures or weak zones that may contribute to tunnel inflow. This assumed failure probability was later incorporated into a pre-posterior analysis, where Bayesian updating was applied to evaluate how the likelihood of failure evolves with the acquisition of new information.

The underlying principle is that gathering additional data reduces uncertainty, thereby increasing the probability of detecting potential failure zones. If the Value of Information Analysis (VOIA) indicates a different preferred alternative compared to the prior analysis, accompanied by a measurable increase in expected benefit, the logical next step is to proceed with field investigations. This process is carried out iteratively, with the model being updated as new data is integrated. The iteration continues until the expected value of the additional information justifies a change in the preferred grouting alternative, measured by a positive difference in expected benefit between the pre-posterior and prior analyses.

Furthermore, validating this hypothesis would require comprehensive, full-scale research supported by adequate time and resources. While this thesis operates within the constraints of the stated hypothesis, alternative scenarios with different probabilities of detection were also explored to assess the sensitivity of the results. This consideration of multiple outcomes aligns with the principles of the observational method and is considered a reasonable approach at the current stage of the study. Evaluating these alternative scenarios enhances preparedness for unexpected conditions during the construction phase, thereby supporting more informed and adaptive decision-making by project stakeholders.

3.3.2 Event probability in the context of modeling

Event probability refers to the likelihood of a specific outcome or condition occurring within a defined system or model. In hydrogeological modeling, it is used to estimate the probability of events such as exceeding groundwater levels, contaminant concentrations, inleakage inside the tunnel, or other critical thresholds.

In probabilistic modeling, events are defined based on conditions or criteria, and their probabilities are assessed using statistical methods, sampling techniques , or analytical approaches. For instance, in a groundwater model, an event might be defined as "the groundwater table exceeds a critical elevation," and the probability of that event is estimated based on model simulations with varying input parameters.

Incorporating event probability in uncertainty analysis
When dealing with parameter uncertainty, event probability provides a quantitative way to assess risk. A large number of model realizations are generated by sampling from uncertain input parameters (e.g., hydraulic conductivity, recharge, porosity). For each realization, the model outputs are compared against predefined event criteria. The fraction of realizations in which the event occurs gives an estimate of its probability.

3.3.3 Conditional probability

Conditional probability describes the chance of an event happening, provided that another event has already taken. In mathematical terms, the conditional probability of event A given event B is written as:

$$P(A \mid B) = \frac{P(A \cap B)}{P(B)} \tag{3.1}$$

3.3.4 Bayesian statistics approach

Classical statistical methods require sufficient measured data to define a probability density function (PDF) and calculate reliable summary statistics such as the mean and variance (Freeze et al., 1990). These methods are limited in early stages of modeling when data are sparse, as confidence in the estimates is low and improves only as more data become available. In contrast, the Bayesian statistical approach enables uncertainty quantification even with limited data. It begins with a prior estimate of the PDF, informed by early measurements, expert judgment, or analogous experience. As new data are collected, Bayes' theorem is used to update the prior, producing a posterior distribution that reflects both prior knowledge and new evidence. Under sparse data conditions, Bayesian estimates may differ significantly from classical ones, but both approaches tend to converge as more data become available.

Bayes' rule, as expressed in Equation 3.2, is employed to update the prior probability (Clyde et al., 2022). Suppose $P(A)$ represents the initial probability of event A occurring. When event B occurs with probability $P(B)$, Bayes' rule allows for the calculation of the posterior probability, or the updated belief about event A, given the occurrence of event B. This updated probability is denoted as $P(A|B)$.

$$P(A|B) = \frac{P(B|A) \cdot P(A)}{P(B)} \tag{3.2}$$

Here, $P(B|A)$ represents the likelihood of observing event B assuming that A is true, while $P(B)$ is defined as shown in Equations 3.3 and 3.4.

$$P(B) = \sum_{a \in A} P(B \cap A) \tag{3.3}$$

$$P(B) = \sum_{a \in A} P(B \cap A) = \sum_{a \in A} P(B|A)P(A) \tag{3.4}$$

Based on the definition of P(B) above, It can be further rewritten as 3.5 as shown below:

$$P(A|B) = \frac{P(B|A)P(A)}{\sum_{a \in A} P(B|A)P(A)} \tag{3.5}$$

In this study, Bayes' theorem is applied to estimate the probability of failure given that no failure has been detected, as shown in Equations 3.6 and 3.7.

$$P(F \mid \neg D) = \frac{P(\neg D \mid F) \cdot P(F)}{P(\neg D)} \tag{3.6}$$

$$P(\neg D) = P(\neg D \mid F) \cdot P(F) + P(\neg D \mid \neg F) \cdot P(\neg F) \tag{3.7}$$

3.3.5 Cost benefit analysis

Cost–Benefit Analysis (CBA) is conducted in two key stages: first during the prior analysis and subsequently within the pre-posterior analysis. In the prior analysis, the objective is to identify the most economically favorable grouting alternative based on the highest *Net Present Value (NPV)*, calculated without considering the benefit of acquiring additional data. In contrast, the pre-posterior analysis extends this approach by incorporating the expected value of new information into the NPV calculation, thereby evaluating how future investigations could influence decision-making. The NPV for each alternative is computed using Equation 3.8:

$$NPV_i = Benefit_i - Cost_i - Risk_i \tag{3.8}$$

Here, $Cost_i$ refers to the direct expense of pre-excavation grouting, while $Risk_i$ accounts for the expected cost of failure. The risk cost is estimated as the product of the probability of failure $P(F)$ and the corresponding cost of failure C_f, i.e.,

$$Risk_i = P(F)_i \times C_f \tag{3.9}$$

This formulation provides a comprehensive measure of the expected performance and financial viability of each grouting strategy under existing uncertainty.

3.3.5.1 Estimation of construction cost

The total cost comprises both construction and consequence components. The construction cost refers to the expenses associated with implementing the grouting process, while the consequence cost accounts for losses or damages incurred if the grouting fails to perform as intended. This study compares two grouting design alternatives that vary in terms of execution quality, specifically, the number of boreholes per grouting fan and the type of grout material employed. Alternative A1 represents a cost-effective option, designed for standard geological conditions and moderate groundwater inflow control. It consists of 20 boreholes per grouting fan, using cement-based grout as the sealing agent. In contrast, Alternative A2 is tailored for more challenging ground conditions where stricter inflow limitations are required. This approach builds upon the A1 design

by incorporating 10 additional boreholes per fan, resulting in a total of 30 boreholes and uses a dual grouting strategy: the original 20 boreholes are grouted with cement, while the 10 supplementary boreholes are treated with silica sol, a low-viscosity chemical grout effective in sealing finer fractures.

To calculate the total grouting cost, the first step involved identifying the lengths of tunnel sections within fractured zones that necessitate grouting. Details regarding these fractured sections are provided in Table 3.4.

Table 3.4: Length of grouting in fracture

Fractures	Length (m)
Geta1	100
Geta2	200
General1	90
General2	170
General3	80
General4	80
General5	120
General6	80

The grouting cost per fan, with each fan having a length of 10 meters, was taken from Zetterlund et al. (2011) and is presented in Table 3.5.

Table 3.5: Specifications of the alternative grouting design and their corresponding cost.

	Alternative 1. Basic grouting design	Alternative 2. Extensive grouting design	Costs
Preexcavation grouting			
Number of boreholes	20	20+10	151000
Type of grout	cement	cement+silica	255000

Table 3.6: Cost Comparison Between Alternative 1 and Alternative 2

S.No	Fractures	Length (m)	Alt 1	Alt 2
1	Geta1	100	1,510,000	2,550,000
2	Geta2	200	3,020,000	5,100,000
3	General1	90	1,359,000	2,295,000
4	General2	170	2,567,000	4,335,000
5	General3	80	1,208,000	2,040,000
6	General4	80	1,208,000	2,040,000
7	General5	120	1,812,000	3,060,000
8	General6	80	1,208,000	2,040,000
Total Estimated Cost (SEK)			**13,892,000**	**23,460,000**

3.3.5.2 Failure cost

Grouting is a critical component in tunnel construction to ensure groundwater control and structural stability. When grouting fails to meet performance criteria, particularly with respect to allowable inleakage, the consequences can be significant, both technically and economically. This section outlines the potential failure outcomes and presents an estimated range of associated costs.

In this study, failure is characterized by the grouting system's inability to reduce groundwater inleakage below the permissible threshold, which is set at 15 liters per minute per 100 meters of tunnel, as specified in Trafikverket (2022). Exceedance of this threshold can trigger a series of negative consequences including remedial work, operational inefficiencies, and regulatory non-compliance.

To simplify this study, it is assumed that both Alternative 1 and Alternative 2 include a provision for post-excavation grouting using silica sol in cases where the pre-excavation grouting alone does not satisfy the required inflow limits. This assumption reflects a commonly used remedial strategy in tunneling projects, where post-grouting serves as a backup to ensure performance targets are met. For the purpose of cost estimation, the cost of post-grouting is set at SEK 105,000 per fan, a value adopted from Zetterlund et al. (2011). Including this step in both alternatives provides a more realistic evaluation of total project costs and highlights the importance of accounting for potential additional measures when grouting performance is uncertain.

4 Results

4.1 Results from hydrogeological simulation model

The Figure 21 illustrates multiple realizations, showing the range of hydraulic conductivity values for general fractures and getå fracture. The exact numbers are presented in the appendix D.1. A triangular distribution was used to generate multiple realizations, as described in the Methods section. The resulting hydraulic conductivity distributions from each realization were compared to the SSR to assess how much they deviated from reality. In this study, "reality" refers to the observed hydraulic head at the observation points along the tunnel alignment.

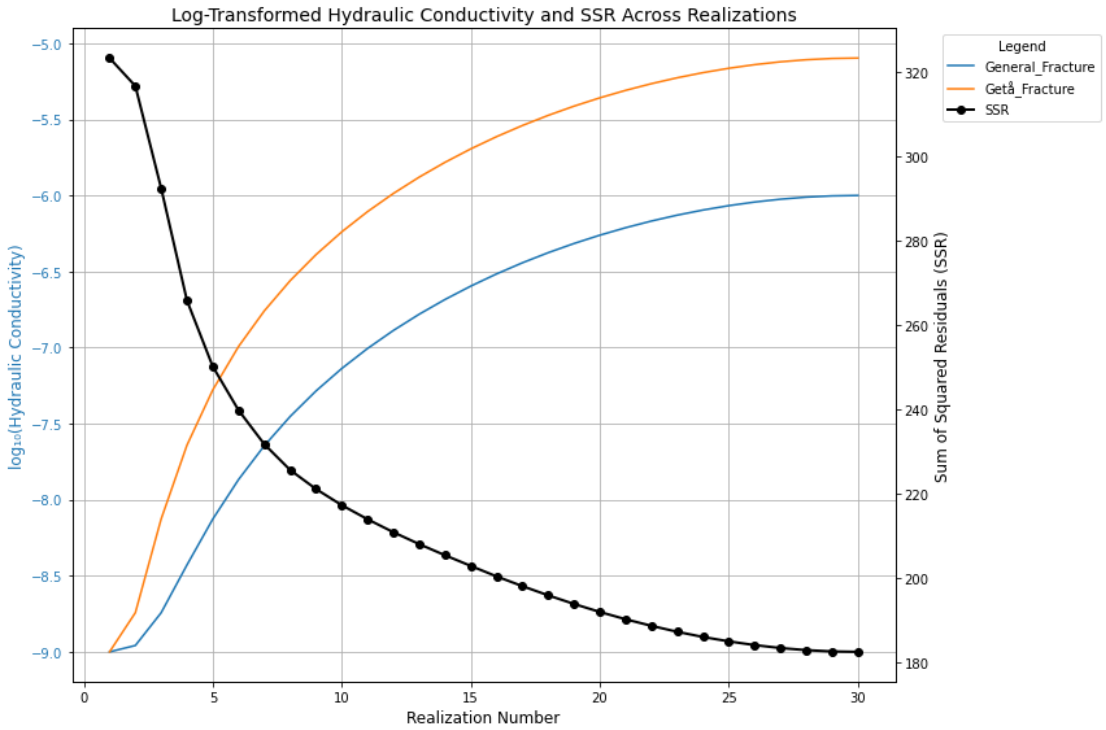

Figure 21: Demonstrating the variability of hydraulic conductivity in distinct areas of structural weakness and SSR comparision.

Figure 21 illustrate the results of a parametric study assessing the sensitivity of the system performance, represented by the SSR value, to variations in the hydraulic conductivity of two major fracture categories: the General Fractures and the Getå Fractures. The hydraulic conductivity values were incrementally increased over 30 realization, ranging from 1.00×10^{-9} m/s to 1.00×10^{-6} m/s for the General Fracture, and from 1.00×10^{-9} m/s to 8.00×10^{-6} m/s for the Getå Fracture.

Increasing the hydraulic conductivity in these fracture zones results in a steady decrease in the SSR value, from around 323 to 183, suggesting an enhancement in model performance or a closer alignment with observed conditions. The rapid drop in SSR values during the early stages of conductivity increase (e.g., scenarios 1–10) suggests a high sensitivity of the system to even modest increases in fracture permeability. Beyond scenario 20, the SSR curve begins to flatten, indicating that the system response becomes

less sensitive to further increases in conductivity at higher values.

This behavior highlights the importance of accurately characterizing fracture zone conductivities, particularly within the lower range, as small underestimations may result in significant misjudgments in predicted performance.

A complementary analysis was conducted by removing an outlier in the original SSR dataset, resulting in a revised sensitivity trend (see Figure 22). The outlier was the observation point '16S115GU', which exhibited a significantly higher residual value compared to other observation points. In this adjusted scenario, the SSR values range from approximately 67 to 55, significantly lower than in the initial analysis. Despite the change in magnitude, the general trend remains: increased hydraulic conductivity in the General and Getå fracture zones corresponds to a gradual decline in SSR, reflecting increasing system performance.

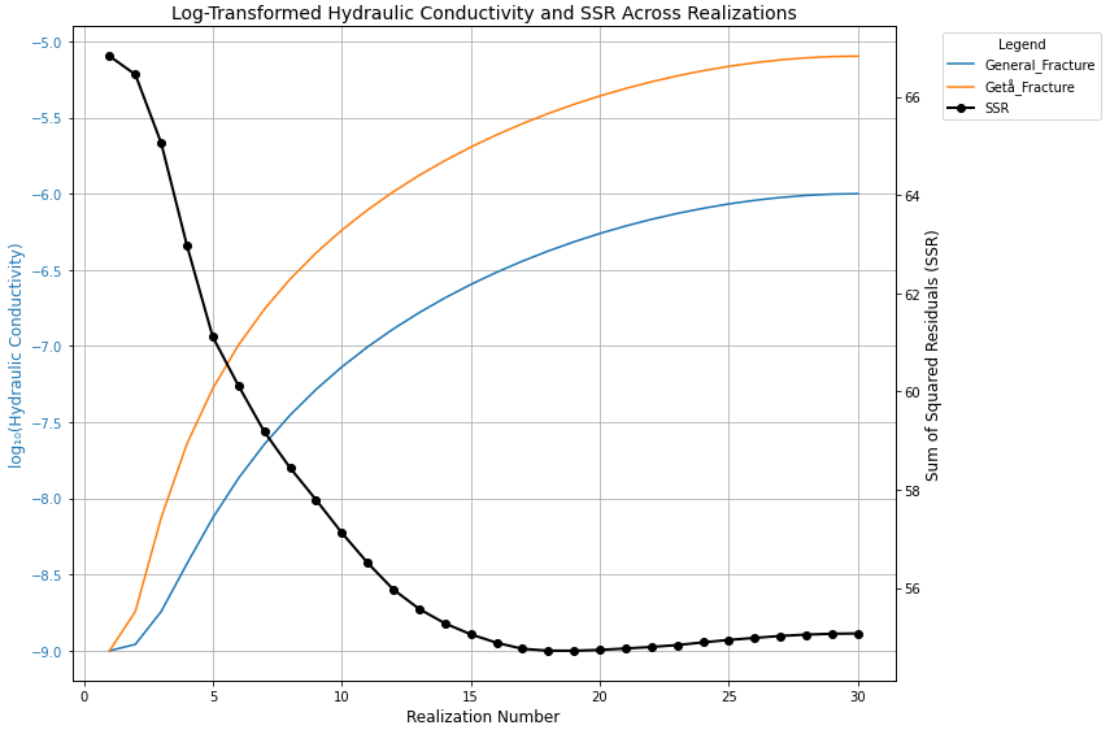

Figure 22: Demonstrating the variability of hydraulic conductivity in distinct areas of structural weakness and SSR comparison after removing the observation point '16S115GU'.

Interestingly, the sensitivity of the system appears reduced in the adjusted dataset, particularly in the higher conductivity range. The SSR values stabilize around 54.7 beyond realization 20, showing a considerably flatter response curve compared to the original. This may suggest that the removed outlier had a disproportionate influence on the sensitivity analysis, especially in the lower conductivity range. The results reinforce the importance of careful data scrutiny and outlier handling in hydrogeological modeling.

Figure 23 presents a detailed analysis of residual variation across all observation points and realizations. The observation point 16S115GU distinctly stands out as an outlier, consistently displaying a much higher range of residual values compared to the rest. Notably, several observation points, including 16S129GU, 17S102GU, and 17HB104,

exhibit an interesting pattern where the simulated head initially overestimates the observed value, then shifts to underestimation, and eventually returns to overestimation. This alternating trend highlights the sensitivity of these locations to parameter changes and suggests potential complexities in local hydrogeological conditions.

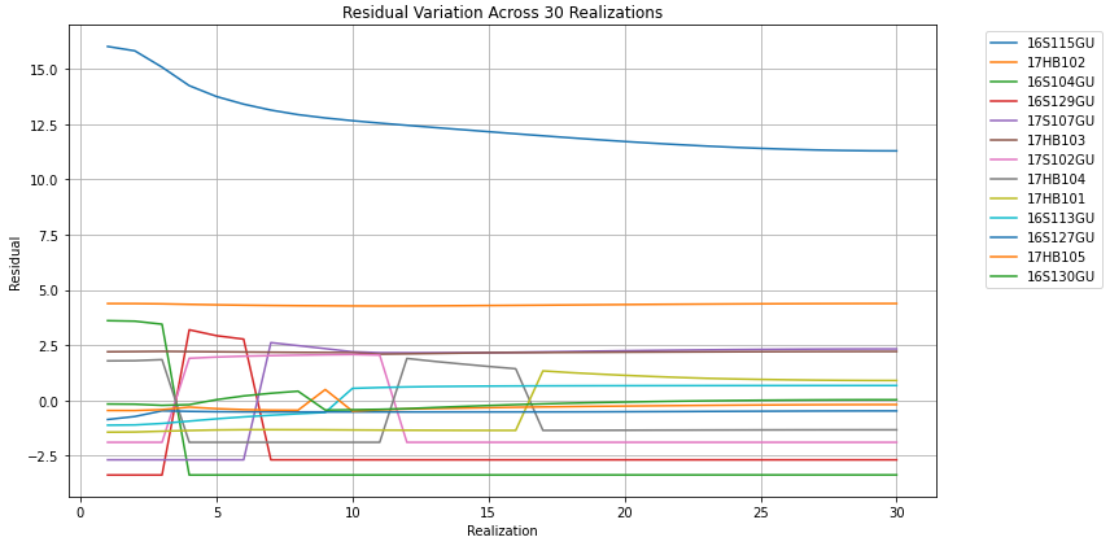

Figure 23: Showing how residuals fluctuate at each observation location and for each realization.

4.1.1 Tunnel without grouting

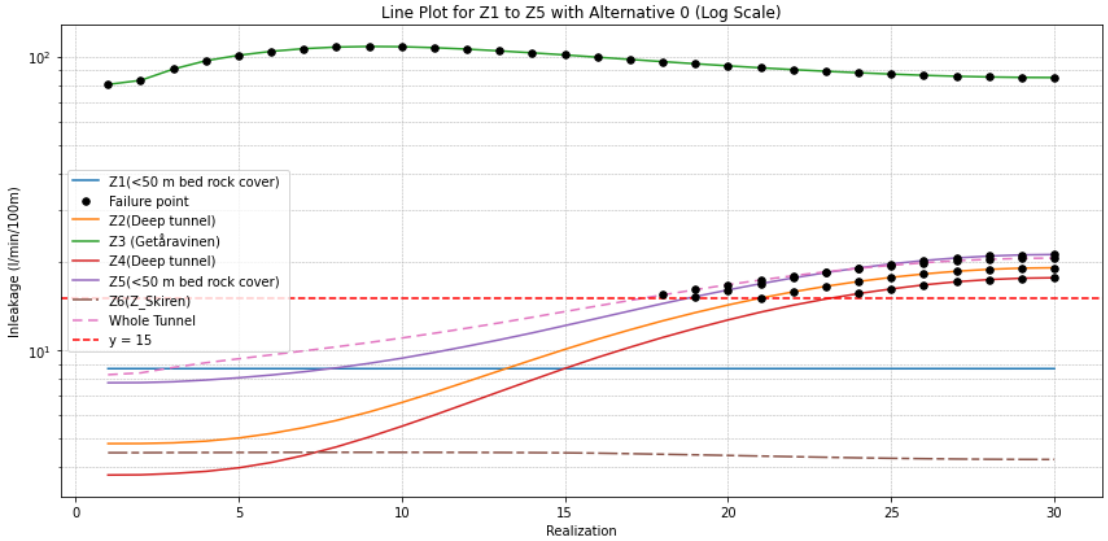

Figure 24: Demonstrating the variability of inleakage inside the tunnel at different zones without grouting

The tunnel inleakage was analyzed under conditions without any grouting measures. The results, presented in Figure 24, show the natural groundwater inflow along the tunnel alignment, which was divided into multiple zones. Inleakage was assessed separately for each zone, providing insights into spatial variations in groundwater inflow.

This baseline scenario helps identify critical sections with higher inflow and serves as a reference for evaluating the effectiveness of future grouting or sealing interventions in specific tunnel zones.

Zone 3, situated near the Getå ravine, emerges as the most critical section, as it exhibits significant inleakage at relatively lower fracture hydraulic conductivities compared to other zones, indicating a higher vulnerability and likelihood of failure in this area. The second most critical zone is at the southernmost end of the tunnel, where the rock cover is less than 50 meters, making it more susceptible to inflow. With further increases in hydraulic conductivity, inleakage also begins in Zone 2 (the northern deep section of the tunnel) and Zone 4 (the southern deep section), suggesting progressive vulnerability in these deeper segments. Lake Skiren is a critical feature in the area, and it is essential to ensure that water from the lake is not draining into the tunnel. The results indicate a constant but minimal level of inleakage inside the section of tunnel close to lake skiren, which remains just above the defined failure threshold of 4 l/min/100m. Considering the tunnel as a whole, the inleakage begins to exceed the failure threshold from realization number 18.

4.1.2 Tunnel with Alternative 1

Initially, the most cost-effective grouting design was analyzed, based on the details provided in the methods section 3.2.3. The results of the model analysis are presented in Figure 25. This evaluation serves as a starting point for assessing the performance of basic sealing strategies and helps identify whether minimal intervention is sufficient to keep inleakage within acceptable limits or if more intensive grouting solutions are required.

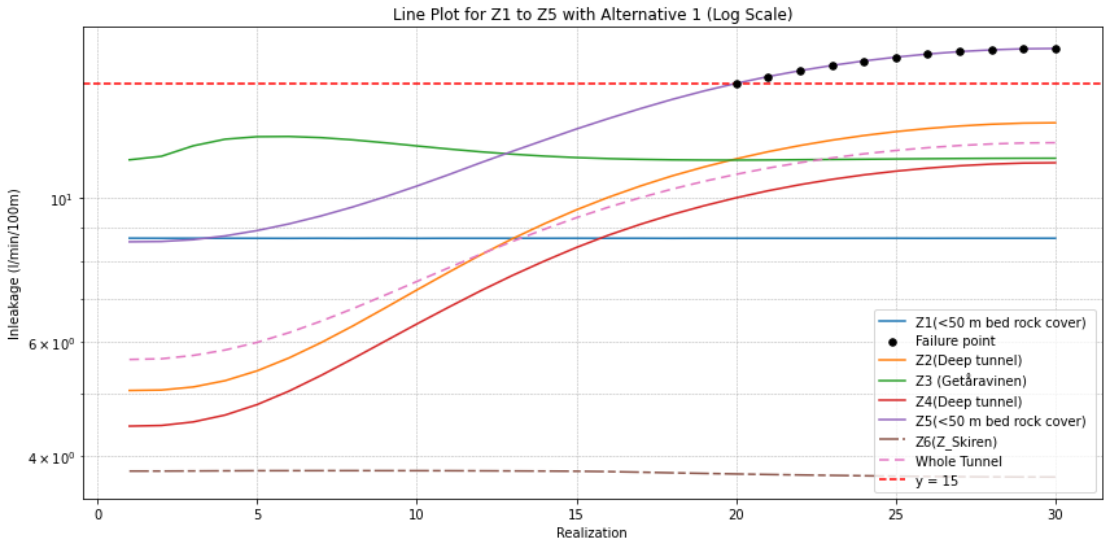

Figure 25: Demonstrating the variability of inleakage inside the tunnel at different zones with alternative 1.

In this scenario, Zone 5, the southern section of the tunnel with a rock cover of less than 50 meters, emerges as the critical area, where inleakage begins to exceed the failure threshold starting from realization 20. In contrast, all other zones remain within the acceptable failure threshold.

4.1.3 Tunnel with Alternative 2

After evaluating the basic, cost-effective grouting strategy, a more advanced and cost-intensive option, Alternative 2, was examined. This design applies a higher grouting quality, as mentioned in Section 3.2.3, targeted at the fracture network similar to A1. The key difference lies in the use of silica-based grout and number of borehole, which offers more effective and durable sealing around the tunnel, enhancing protection against inleakage in critical areas. The aim of this alternative is to significantly reduce inleakage in areas where the minimal design (Alternative 1) was found to be insufficient, such as Zone 5.

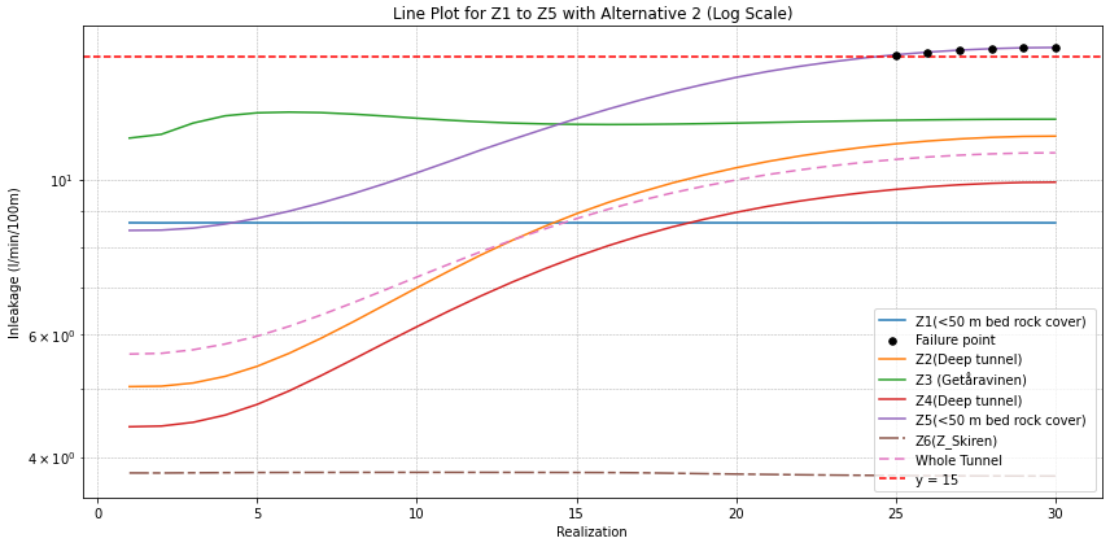

Figure 26: Demonstrating the variability of inleakage inside the tunnel at different zones with alternative 2

The results of the model analysis for Alternative 2 are presented in Figure 26 . Compared to Alternative 1, this design achieves a substantial reduction in inleakage across all tunnel zones, keeping the inflow well below the failure threshold. Although more expensive, this solution provides a higher degree of reliability and may be justified in sections of the tunnel where environmental protection, safety, or long-term durability are critical concerns.

4.1.4 Zone-wise analysis of groundwater inleakge

A zone wise comparision of inleakage for the three grouting altenatives (A0, A1, and A2) is presented in Figure 27. The inleakage value are plotted on a logarithmic scale across multiple tunnel sections and for the entire tunnel. A critical inflow threshold of 15l/min/100m is indicated to assess the acceptability of each alternative. In Zone Z1, where the bedrock is less than 50 meters, all alternatives remained well below the threshold and with same inleakage. The reason behind the same inleakage is the absence of fracture in this zone, so no effect of grouting was seen as well.

In the deeper tunnel sections, specifically Zone 2 (Z2) and Zone 4 (Z4), Alternative A0 showed a sharp rise in inflow as the hydraulic conductivity of fractures increased, eventually exceeding the allowable limits. In particular, Z2 began to surpass the threshold starting from realization 21, while Z4 exceeded the limit from realization 24 onward.

In contrast, Alternatives A1 and A2 demonstrated more stable performance under the same conditions, reflecting the effectiveness of improved grouting measures. As expected, the application of more extensive grouting in led to a noticeable reduction in inleakage in both Zone 2 and Zone 4.

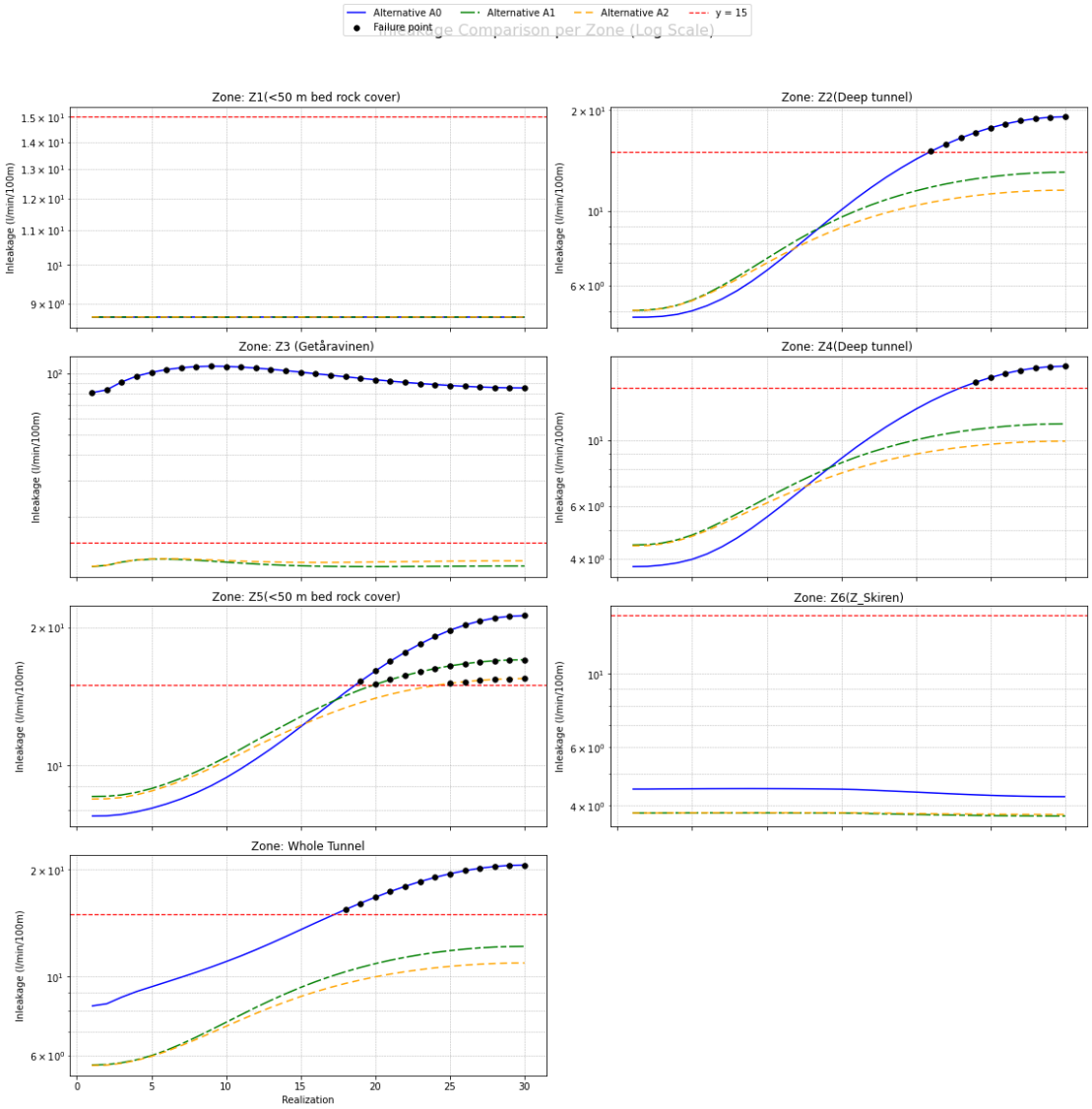

Figure 27: Illustrating assessment of inleakage variation by alternative across multiple zones

Zone Z6 (Z_Skiren) exhibited consistently low inflow across null alternatives, indicating either favorable geological conditions or naturally low rock permeability in that section. However, due to its proximity to Lake Skiren, a site of national interest, stricter inflow limits have been enforced in this zone, as outlined in Section 2.5. To safeguard the lake from potential drainage into the tunnel, more rigorous sealing measures are recommended. In this context, extensive sealing solutions, such as prefabricated sealing segments, are advised to ensure that the grouting performance modeled reflects the level of protection required for this environmentally sensitive area.

Zone 3 (Getåravin) represents the most critical and vulnerable section of the tunnel alignment, located between two major fractures Getå1 and Getå2. This segment is

characterized by elevated hydraulic conductivity, which results in significantly higher inflow. In Alternative A0, the inflows reached 108 l / min / 100 m, consistently exceeding the permissible threshold in all realizations. These findings highlight the need for intensive sealing measures, such as the use of prefabricated sealing segments, to effectively reduce hydraulic conductivity in this area, as reflected in the modeling approach used in this study.

When evaluating leakage across the entire tunnel, Alternative A0 resulted in the highest total inleakage, reaching up to 20.61 l/min/100m. The overall inflow for A0 began to exceed the allowable threshold from realization 18 onward. In comparison, Alternatives A1 and A2 consistently maintained inleakage below the threshold throughout all realizations. As expected, the more expensive grouting strategy in Alternative A2 outperformed the others, achieving the lowest inleakage, with a maximum of 10.92l/min/100m, while A1 recorded a slightly higher peak of 12.16 l/min/100m.

In Zone Z5, the inleakage results show a distinct contrast between the three alternatives. Alternative A0, which involves no grouting, exhibits a significant rise in inleakage across many realizations, with several values exceeding the critical threshold of 15 l/min/100 m. This indicates that the zone contains permeable fractures that allow considerable water ingress in the absence of sealing measures. Alternative A1, utilizing standard grouting, shows better performance than A0 by lowering inleakage levels; however, from realization number 20 onward, the values begin to approach the threshold. The most effective outcome is seen with Alternative A2, which employs an enhanced grouting design. Prior to realization number 25, Alternative A2 consistently keeps inleakage levels significantly below the threshold, demonstrating the effectiveness of intensive grouting in hydraulically vulnerable zones such as Zone Z5.

4.1.5 Sealing reliability

In the design of underground structures such as tunnels, especially in fractured rock environments, evaluating the reliability of sealing systems is a critical aspect of ensuring long-term performance. A key consideration is the probability of failure, P(F), which in this context refers to the likelihood that groundwater inflow into the tunnel exceeds the allowable threshold due to insufficient sealing.

For tunneling projects affected by complex hydrogeological conditions, potential failure mechanisms typically involve two main components: one associated with the engineered system, such as grouting materials and methods, and the other related to the natural variability and uncertainty of the surrounding hydrogeological environment (Freeze et al., 1990). Each of these components contributes to the overall uncertainty in achieving the desired sealing performance.

For instance, the engineered component may fail due to inadequate grout spread, imperfect contact with rock fractures, or deterioration of sealing materials over time. On the other hand, the hydrogeological component includes uncertainties in fracture distribution, aperture, connectivity, and the hydraulic conductivity of the rock mass. Even with well-executed grouting, high-permeability pathways or unsealed minor fractures may lead to local zones of excessive inleakage.

For the purpose of this thesis, only Zone 5 was selected for detailed analysis, as it is the only section that clearly demonstrates a distinct contrast among the three alternatives in terms of uncertainty related to failure. The probability of failure in this zone is assessed

based on the probability distribution function, as illustrated in the following.

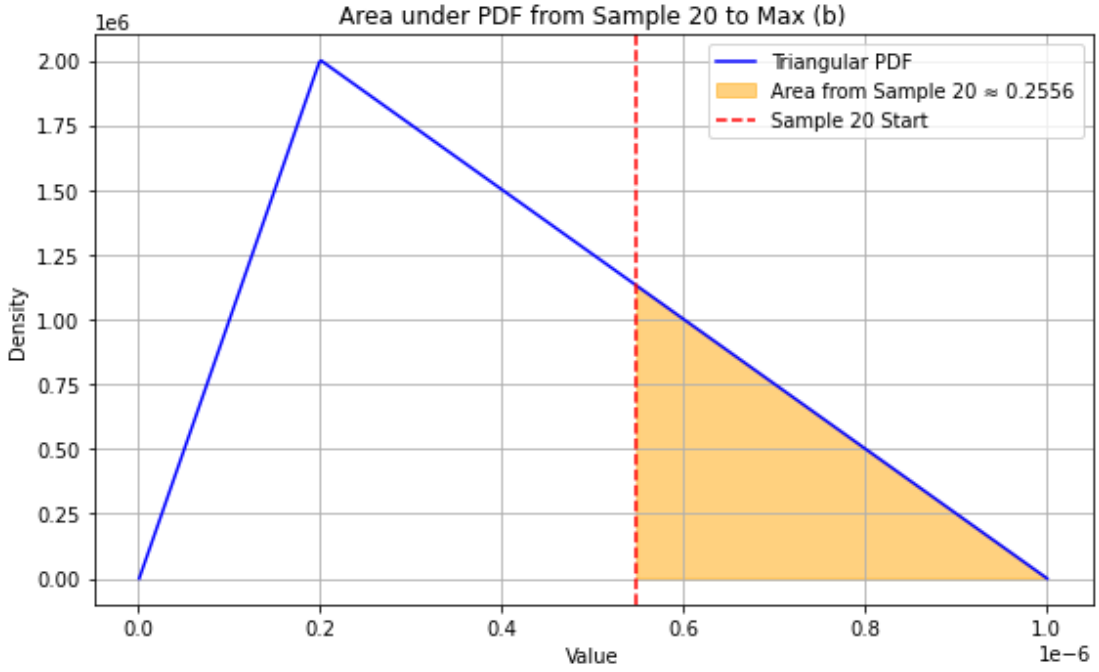

Figure 28: Illustration of the probability of failure for alternative 1

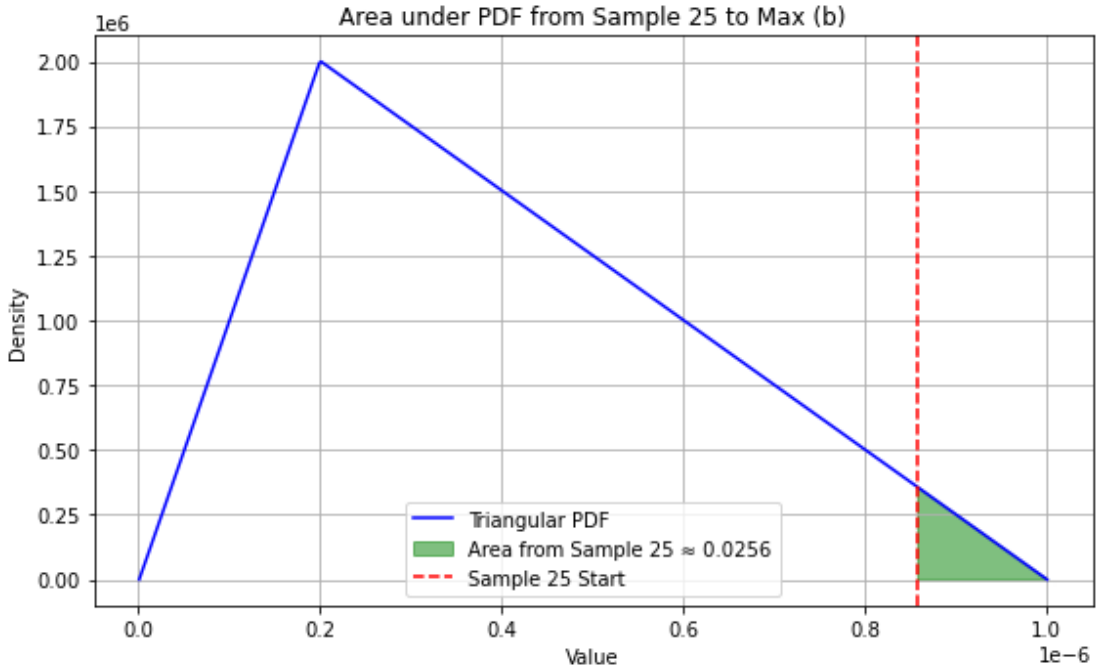

Figure 29: Illustration of the probability of failure for alternative 2

Based on the Figure 28 and 29, it can be inferred that the probability of failure for Sealing Alternative 1 is approximately 25.56%, while Sealing Alternative 2 exhibits a significantly lower failure probability of around 2.56%. This suggests that the more robust and cost-intensive design of Alternative 2 offers a higher level of reliability in

maintaining acceptable inleakage levels. The reduction in failure probability highlights the effectiveness of enhanced grouting measures, such as the use of silica-based grout and a higher number of bore hole, in better controlling groundwater ingress under uncertain hydrogeological conditions. These findings underscore the value of incorporating probabilistic analysis in the evaluation of design alternatives, especially when dealing with fractured rock environments.

4.2 Results from VOIA

4.2.1 Prior Analysis

To inform the evaluation of tunnel grouting strategies, a prior analysis was conducted comparing two alternatives:

- A1: Standard grouting – a baseline design with standard sealing.
- A2: Expensive grouting – a more robust and costly design intended to minimize failure risk.

This analysis assumed zero direct economic benefit for both alternatives, focusing instead on construction cost, probability of failure, and potential failure consequences. Each alternative was evaluated based on its Net Present Value (NPV) and comparision is present in Table 4.1 :

Table 4.1: Prior Analysis Results for Grouting Alternatives A1 and A2

Parameter	**Alternative A1: Standard grouting**	**Alternative A2: Expensive grouting**
Construction Cost [kr]	$-1,208,000$	$-2,040,000$
Probability of Failure (P_f))	25.56%	2.56%
Cost of Failure [kr]	$-840,000$	$-840,000$
Net Present Value (NPV) [kr]	$-1,422,700$	$-2,061,500$

The calculation are illustrated in Figure 30 for more insigt into study.

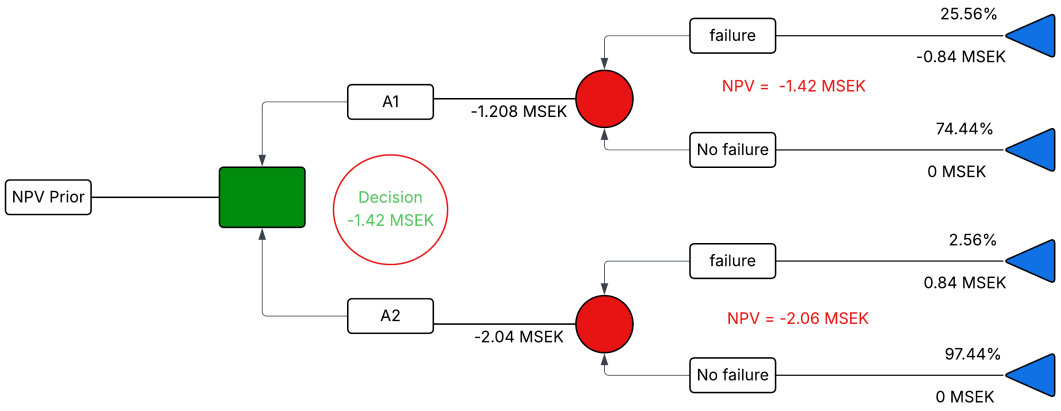

Figure 30: Illustration of Prior analysis

Despite the much lower failure probability of Alternative A2, its significantly higher construction cost results in a more negative NPV. In contrast, the standard Alternative (A1), although riskier, leads to a less negative NPV and is therefore economically preferable under the prior assumptions.

This prior analysis serves as the baseline comparison between the two alternatives before incorporating additional measurements or updated knowledge in a posterior analysis. It highlights the classic trade-off in hydrogeological design between construction costs and failure risks. Based on the prior probabilities and cost parameters, A1: Standard grouting alternative emerges as the better choice.

4.2.2 Pre posterior Analysis

In the presence of uncertainty regarding the performance of sealing systems in fractured rock tunnels, decision-making can benefit from evaluating whether additional investigations (e.g., targeted hydraulic tests or pilot grouting trials) would improve the reliability of the selected alternative. A pre-posterior analysis is performed to determine the expected benefit of gathering new information before committing to a sealing strategy.

This analysis accounts for the reliability of the investigative method by incorporating conditional probabilities such as $P(D|F) = 0.80$, representing the probability of detecting a failure when it exists, and $P(D|\neg F) = 0.00$, representing the probability of detecting failure when it does not exist (i.e., a false positive is not expected). Conversely, $P(\neg D|F) = 0.20$ reflects the probability of not detecting failure despite its presence (false negative), and $P(\neg D|\neg F) = 1.00$ assumes a true negative.Using the law of total probability, the marginal probabilities for detection and non-detection of failure can be derived.

- $P(D)$: Probability that failure is detected

$$P(D) = 20\%$$

- $P(\neg D)$: Probability that failure is not detected

$$P(\neg D)) = 80\%$$

4.2.2.1 Branch 1: Given that failure is detected

When failure is detected, the preposterior probability of failure becomes same as prior analysis. The results for this branch is presented in table 4.2:

Table 4.2: Comparison of Alternatives A1 and A2

Parameter	**Alternative A1: Standard grouting**	**Alternative A2: Expensive grouting**
Construction Cost [kr]	$-1,208,000$	$-2,040,000$
Probability of Failure (P_f)	25.6%	2.56%
Cost of Failure [kr]	$-840,000$	$-840,000$
Net Present Value (NPV) [kr]	$-1,422,700$	$-2,061,500$

Best Alternative: A1

4.2.2.2 Branch 2: Given that failure is not detected

If no failure is detected, the pre-posterior probability of failure for A1 drops to 6.4% based on Bayes' theorem as shown below:

We have:

$$P(\neg D \mid F) = 0.20, \quad P(D) = 0.2, \quad P(\neg D) = 0.80$$

Substituting the values:

$$P(F \mid \neg D) = \frac{0.20 \cdot 0.2556}{0.80} = \frac{0.052}{0.80} = 0.064 = 6.4\%$$

Likewise, for Alternative 2, the pre-posterior probability $P(F \mid \neg D)$ is 0.5%, and the outcome for this scenario is shown in Table 4.3. The graphical illustration of Bayesian updating for alternative 1 is presented in Figure 31.

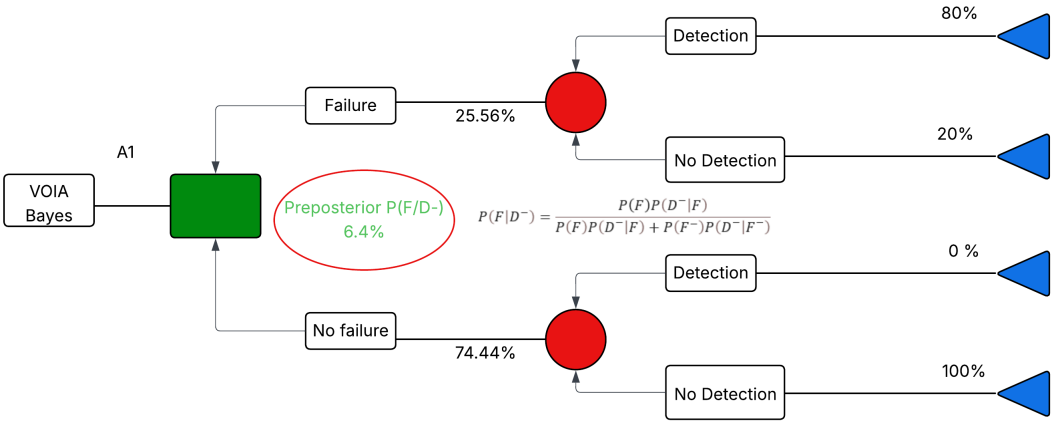

Figure 31: Illustration of Bayesian updating

Table 4.3: Comparison of Alternatives A1 and A2

Parameter	**Alternative A1: Standard grouting**	**Alternative A2: Expensive grouting**
Construction Cost [kr]	$-1,208,000$	$-2,040,000$
Probability of Failure (P_f)	6.4%	0.5%
Cost of Failure [kr]	$-840,000$	$-840,000$
Net Present Value (NPV) [kr]	$-123,526,853$	$-2,044,391$

Best Alternative: A1

The graphical illustration of pre-posterior analysis is presented in Figure 32

4.2.2.3 Pre-Posterior expected value and decision

The weighted expected Net Present Value (NPV) of the standard alternative, considering both the probabilities of detection and non-detection, is calculated to be –1,294,843 kr.

This represents an improvement compared to the prior analysis NPV of –1,422,704 kr, indicating a positive Value of Information (VOI) of 127,861 kr.

Although the VOI demonstrates that acquiring additional information through investigation could improve decision confidence, it does not lead to a change in the preferred alternative, which remains Alternative A1. As a result, the practical benefit of pursuing further investigation is limited, since the decision outcome would remain the same. Therefore, from a cost-effectiveness perspective, additional investigation is not recommended, as the VOI does not outweigh the resources required to obtain new data, nor does it shift the decision-making outcome in this particular case.

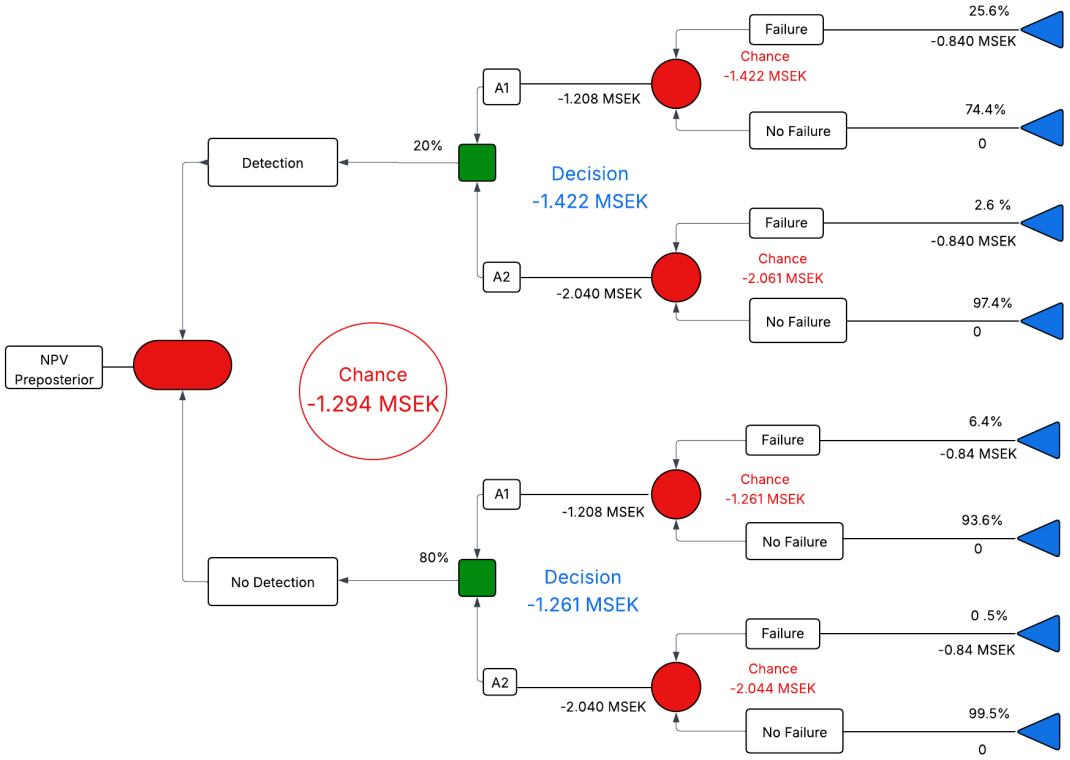

Figure 32: Illustration of Preposterior analysis

4.2.3 Sensitivity Analysis

4.2.3.1 Effect of varying hydrogeological test method reliability

For the purpose of this thesis, it was assumed that the probability of detecting a failure, given that a failure exists, denoted as $P(D \mid F)$, is 80%. This assumption served as a baseline for the pre-posterior analysis. However, to better understand the influence of this parameter on the overall decision-making process, a sensitivity analysis on the reliability of the hydrogeological test methods is warranted. By varying the assumed detection probability, it is possible to explore how the outcomes, such as the probability of failure, expected value of information (VOI), and recommended alternatives, respond to changes in investigative reliability.

At the current stage of the study, there is no well-defined or empirically validated method for deriving this probability without conducting comprehensive field investi-

gations or developing a statistically robust framework. The actual detection efficiency may depend on multiple factors, such as the type of test (e.g., slug tests, water loss tests), site-specific conditions, instrumentation precision, and operator experience. Since deriving these values is beyond the scope of this work, the selected assumption acts as a reasonable proxy for demonstration purposes.

Nevertheless, incorporating a range of detection probabilities into the analysis enables the identification of threshold values at which the decision outcome might change. A sensitivity analysis was conducted by varying the assumed detection probability, $P(D \mid F)$, from 0% to 100%. The results, shown in Figure 33 and 34, indicate the corresponding changes in the pre-posterior probability of failure given non-detection, $P(F \mid \neg D)$, the expected Value of Information (VOI), and the weighted expected value for best alternative which in this case A1.

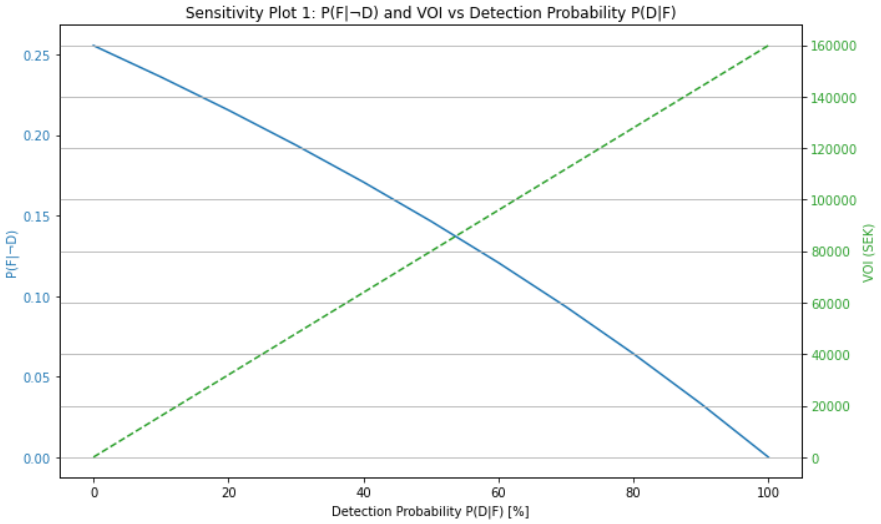

Figure 33: Illustration of variation of VOI and P(F|-D) with variation of test method reliability

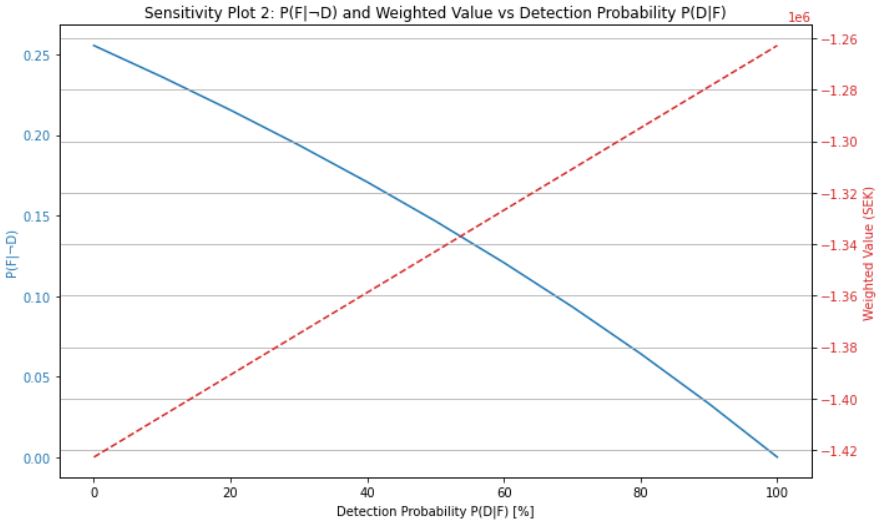

Figure 34: Illustration of variation of NPV of best alternative (A1) after pre-posterior analysis and P(F|-D) with variation of test method reliability

The analysis shows a clear trend: as the probability of detecting a failure when it is present increases, the posterior probability of failure given no detection decreases, leading to a higher VOI and a more favorable (less negative) weighted NPV. For example, increasing $P(D \mid F)$ from 0% to 100% reduces $P(F \mid \neg D)$ from 25.56% to 0%, while the VOI increases linearly to 159,826 SEK.

In this analysis, even when the detection probability $P(D \mid F)$ was varied from 0% to 100%, the preferred alternative remained unchanged, Alternative 1 consistently yielded the highest expected benefit across all scenarios. As a result, no clear threshold could be identified beyond which the additional investigations would lead to a different decision. This suggests that, under the current assumptions and cost structure, further data collection does not significantly shift the balance between alternatives, and therefore, may not be justifiable from a decision-making perspective. Nonetheless, this finding underscores the importance of performing sensitivity analyses to verify the robustness of conclusions against varying levels of investigative reliability.

4.2.3.2 Effect of increasing cost of failure on value of information

A sensitivity analysis was conducted to investigate the impact of varying the cost of failure on the calculated Value of Information (VOI) for the selected alternatives. The cost of failure was progressively increased, ranging from 0.84 Mkr up to 12.6 Mkr, to examine how the relative benefit of additional information changes with higher potential losses.

The results, illustrated in Figure 35, show that the VOI initially increases with the cost of failure. During this initial increase, the preferred alternative remains unchanged between prior and pre-posterior analyses. As a result, the VOI does not justify additional investigation, and no further information acquisition is recommended in this range.

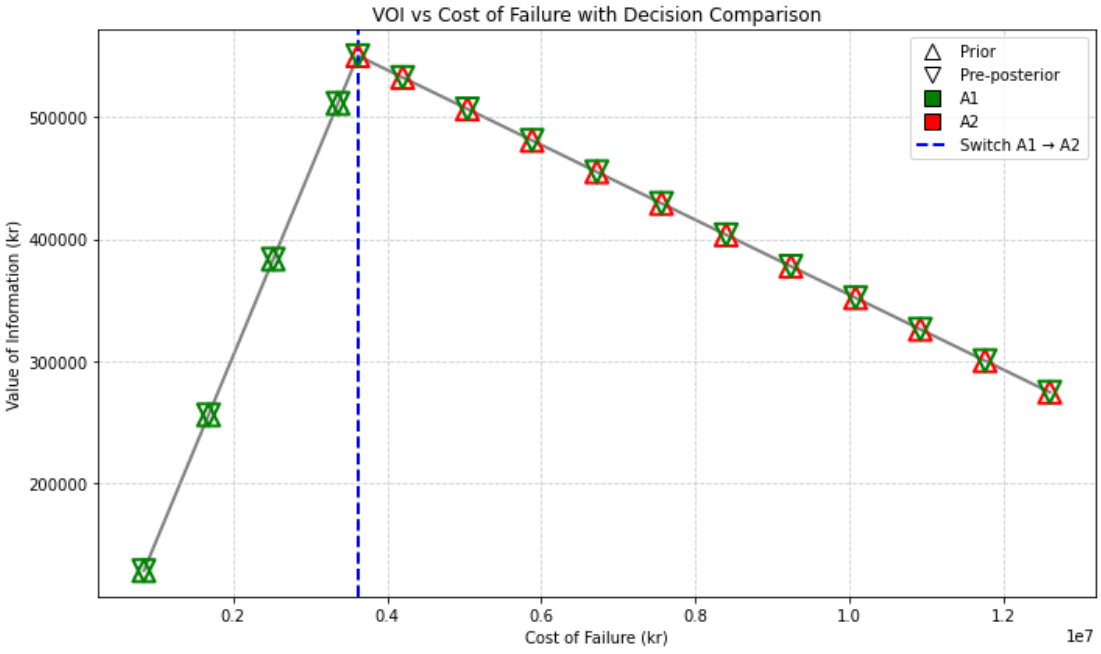

Figure 35: Illustration of variation of VOI and decision alternative with variation of failure cost.

At the peak of the VOI curve, corresponding to a cost of failure of 3,617,880 kr, a critical transition occurs: the preferred alternative changes between prior and pre-posterior analyses. This indicates that additional information could influence the decision, though the VOI decreases slightly beyond this point. The decline in VOI after the peak indicates that once the decision has changed, further increases in the cost of failure lead only to a reduced value of information.

5 Discussion

5.1 Hydrogeological model

5.1.1 Model validation and uncertainty management

The performance of the hydrogeological model was assessed by comparing simulated and observed groundwater heads. While the majority of observation points showed acceptable residuals, observation point 16S115GU, located near the Getåravin, consistently exhibited high residuals across realizations. This suggests potential misrepresentation of local geology or boundary conditions that could not be resolved by parameter adjustments alone. These discrepancies emphasize the need for more localized data collection or improved conceptual modeling in areas of complex hydrogeology.

In addition to head comparisons, incorporating discharge data could provide an alternative means to validate model realizations. Since discharge reflects flow conditions rather than head alone, it could enhance the robustness of the validation process, especially in zones where fracture connectivity dominates inflow behavior.

5.1.2 Spatial heterogeneity of hydraulic conductivity

The probabilistic treatment of hydraulic conductivity in this study, using triangular distributions, was an important step in representing parameter uncertainty. However, spatial variability within and between geological units was not explicitly incorporated. In the current modeling framework, all fractures within the same category were assigned identical hydraulic conductivity values and represented the uncertainty of the total K of the fracture by a triangular distribution. In reality, this assumption oversimplifies natural conditions, fractures of the same geological classification may still exhibit markedly different permeabilities due to factors such as aperture variability, degree of weathering, and the presence of fracture-filling materials like clay, silt etc.

Moreover, even within a single fracture, hydraulic conductivity can vary along its length, influenced by local mineral infill, deformation, and flow channeling. This intrinsic heterogeneity, if ignored, can result in under- or overestimation of flow and inflow predictions in sensitive tunnel sections.

5.1.3 Thickness of grouted zone

In reality, the thickness of the grouted zone is not uniform, even though it is modeled as constant. The actual grout penetration length tends to be greater in fractures with wider apertures and shorter in narrower ones. Additionally, the effective thickness of the grouted zone may be less than the assumed model thickness in cases where certain fractures are not fully sealed. Incomplete grouting can occur when grout boreholes do not intersect the fractures along their planes. Moreover, the presence of clay-filled fractures can further hinder grout penetration, as the clay acts as a barrier that prevents the grout from effectively entering and sealing the fracture network. These factors could lead to a discrepancy between the expected and actual performance of grouting in the field, as the assumptions used in the model may oversimplify the complex and variable nature of real geological conditions.

5.1.4 Critical zones

Two tunnel sections, beneath lake Skiren and near Getåravin, were identified as the most hydrogeologically sensitive areas. In the case of lake Skiren, even minimal leakage poses a significant risk of ecological disturbance. Similarly, the Getåravin zone, bounded by major fracture zones, demonstrated consistently high inleakage and was identified as the most failure-prone area. These zones require enhanced sealing strategies and could serve as targets for more detailed site investigations in future work.

5.1.5 Modelling grouting effect

At this stage of the study, there is insufficient information to accurately quantify the impact of grouting on hydraulic conductivity, specifically, to what extent it reduces conductivity within fractured rock. In this analysis, grouting was simplified by assigning two fixed hydraulic conductivity values, which may not reflect real-world conditions. A more comprehensive investigation is necessary to establish the relationship between the characteristics of the deformation zone, the grouting technique employed, and the type of grout material used.

The study by Zetterlund et al. (2011) also explored the use of Value of Information Analysis (VOIA) in the context of grouting alternatives. However, it did not delve deeply into the specific impact of grouting on hydraulic conductivity. Instead, the focus was on quantifying the uncertainty associated with the likelihood that grouting would fail to adequately seal fractures. A beta distribution was employed to represent this uncertainty, allowing for probabilistic assessment rather than a detailed mechanistic evaluation of conductivity reduction. While this approach is useful for decision-making under uncertainty, it highlights the need for further research to directly link grouting practices with changes in hydraulic conductivity in fractured rock environments.

A key aspect of the study by Zetterlund et al. (2011) was the reliance on expert judgment to estimate the probability of successful pre-grouting. Experts provided input based on prior experience, geological conditions, and expected grout performance to inform the likelihood that the fractures would be adequately sealed. The success rates provided were 60% for cement-only grouting and 90% for grouting using a combination of cement and silica sol. In comparison, the success rates observed in our study were notably higher, 74.6% for cement-based grouting and 97.4% when silica-based grouting was used as a supplement. This highlights that the expert-based estimates in Zetterlund et al. (2011) were more conservative than the outcomes observed in our case.

In addition, the paper incorporated risk cost, which accounted for the potential expenses incurred if the initial grouting fails. These costs include those associated with post-excavation grouting and the construction of drainage systems, both of which may be necessary to achieve acceptable inflow conditions.

5.1.6 Coupled rock-grout behavior in uncertainty analysis

Instead of assuming a constant value, the hydraulic conductivity of the grouted zone can be varied as a function of the surrounding rock's hydraulic conductivity, reflecting more realistic field behavior. One way to implement this is by fixing a sealing factor ratio that defines the efficiency of grouting relative to the host rock permeability. For each realization in the analysis, a different grouted hydraulic conductivity can be assigned based on the corresponding rock properties. This approach allows for a more dynamic

and representative model, enabling multiple simulations to evaluate the reliability of the engineering design under varying geological conditions.

5.1.7 Exploration of new alternative

The analysis can be further refined and extended by evaluating a broader range of alternative grouting designs. The current results indicate that the selected grouting strategy successfully limits water leakage below the failure threshold across all tunnel sections, except in Zone 5, where the inflow still exceeds the acceptable limit. This suggests that the existing design may be overly conservative in some zones and can be optimized further.

Future development could involve optimizing the grouting layout, such as reducing the number of boreholes in zones where the inflow is already well controlled, thereby lowering costs without compromising performance. Conversely, more targeted or intensified grouting could be considered in problematic zones like Zone 5. Incorporating variable design parameters, including borehole spacing, grout type, injection pressure, and fan arrangement, could help tailor the grouting strategy to local geological conditions and improve both efficiency and effectiveness of the sealing process.

5.1.8 Graphical user interface (GUI)

Using a graphical user interface (GUI) such as ModelMuse limited the efficiency and continuity of iterative model runs compared to a script-based approach. Since a major focus of this study involves the uncertainty of hydraulic conductivity in fractures, multiple model runs were required across a wide range of conductivity values. Performing these runs manually in ModelMuse proved to be a tedious and time-consuming task, as each change in the dataset required manually updating inputs and extracting outputs, particularly the leakage estimates across different tunnel sections.

5.1.9 Steady state model

The variation in the water table was not accounted for in this study, despite being a critical parameter that can significantly influence tunnel inflow. Fluctuations in the water table, whether seasonal or induced by nearby construction or groundwater abstraction, can alter hydraulic gradients and, consequently, the rate and distribution of inleakage. Ignoring these variations may lead to an underestimation or overestimation of actual inflow conditions, particularly in areas where groundwater levels are dynamic.

5.1.10 Drawdown in groundwater level as failure criteria

For further analysis, comparison observations can be employed to evaluate drawdown differences between the base model and a model that includes external stress, such as tunnel construction. Each comparison can utilize different realizations of the model. Failure criteria are defined based on thresholds for specific geological units, such as rock or clay, below which conditions are considered unacceptable. Moreover, given that Lake Skiren is a critical feature in the area, monitoring potential declines in its water level is particularly important. Therefore, comparing water levels before and after tunnel excavation provides a basis for assessing possible failure.

5.1.11 Triangular distribution and its implications

The use of triangular distribution to represent uncertainty in hydraulic conductivity of fractures was a practical choice in this study, especially in the absence of extensive site-specific data. This distribution allows for intuitive parameterization using a minimum, maximum, and most probable value, making it suitable for conceptual and early-stage decision support modeling. However, an important implication observed during the analysis is that in several realizations, the sampled hydraulic conductivity of fractures was lower than the assumed grouted hydraulic conductivity. This scenario suggests a paradox where grouting may appear to worsen rather than improve the permeability conditions. While such outcomes are artifacts of simplified modeling assumptions, they underline the limitations of using a fixed grouted conductivity across a broad uncertainty range. In reality, sealing interventions should not increase system permeability. Therefore, future work could benefit from dynamically linking grouted hydraulic conductivity to the natural rock conditions, e.g., via a sealing factor or probabilistic function, thereby preventing unrealistic cases and improving model robustness. This refinement would ensure that the grouting model better reflects practical field performance across varying geological settings.

5.1.12 During construction

Monitoring during the construction is more detailed than in the preliminary investigation, actual hydraulic conductivity of grouting can only possible to determine during this stages using the control hole. It is also possible that the hydraulic conductivity of grouted rock mass can be higher than the ungrouted rock mass beacause of measurement method. Since the ungrouted rock mass is oriented in single direction and there is high chance of missing the fracture but control hole is oriented in different direction thus higher possibility that the control holes might hit a more water bearing fracture.

5.2 VOIA

5.2.1 Failure criteria and sensitivity

Failure criteria play a crucial role in the Value of Information Analysis (VOIA), as they directly influence the assessment of whether an alternative meets regulatory or performance requirements and consequently the risk cost. Currently, the absence of an established or approved failure criterion introduces significant uncertainty in decision-making. Even a slight adjustment in the threshold can lead to entirely different conclusions. For example, increasing the failure threshold slightly may result in neither alternative being classified as a failure, suggesting both are acceptable with no risk cost. Conversely, tightening the criterion to a lower value, such as around 13 l/min/100m, would render both alternatives inadequate, as they would fail to meet the necessary legal or performance standards and incur higher risk cost. This sensitivity underlines the importance of clearly defining and justifying the failure criteria in VOIA.

5.2.2 Quality of investigation campaign

In this study, the quality investigation campaign, expressed as the conditional probability of detecting a failure if one exists, $P(D|F) = 0.8$, was assumed solely for the convenience of illustrating the Value of Information Analysis (VOIA) framework. This value was not derived from empirical measurements, literature sources, or expert judg-

ment, and should therefore be treated as a placeholder rather than a definitive estimate of actual investigative reliability.

5.2.3 Importance of investigation cost

While this study did not explicitly incorporate the cost of additional investigations into the analysis, it is important to consider this aspect when applying the Value of Information (VOI) framework. If the expected value of information (EVOI) substantially exceeds the cost of performing an investigation, it becomes economically justified to conduct further data collection. Such investigations should continue iteratively until the EVOI drops below the marginal cost of acquiring new information, indicating that additional data would no longer offer a sufficient decision-making benefit.

Each iteration should involve updating the hydrogeological model to reflect the newly acquired data, thereby improving both the prior analysis and subsequent VOIA loops. This adaptive approach not only enhances the accuracy of the model but also supports more informed and cost-effective decisions under geological uncertainty. It aligns with the principle that the value of further investigation lies not just in reducing uncertainty, but in how that reduction translates into better project outcomes and risk management.

5.2.4 Synergy between VOIA and observational method

The observational method, as outlined in Eurocode 7, provides a structured and adaptive framework for managing geotechnical uncertainty, particularly in complex underground construction projects such as tunnels. Originally introduced by Peck (1969) and further developed in literature and standards (e.g., SIS, 2005), the method emphasizes continuous updating of the geological model and design modifications during construction. This approach is especially relevant when ground conditions are difficult to predict based on limited pre-investigation data. In essence, it reflects a philosophy of "design as you go," using real-time observations to refine both the understanding of subsurface conditions and the engineering response. This is closely aligned with the rationale behind the Value of Information Analysis (VOIA), which seeks to quantify the benefit of acquiring additional data prior to decision-making. VOIA supports the early stages of the observational method by helping prioritize where and how much to invest in site investigations. By identifying areas with the greatest impact on decision uncertainty, such as in zone 5 in our study, enables more informed choices about pre-investigation programs and potential contingency designs. Integrating VOIA with the observational method can therefore improve both the planning and execution phases of geotechnical design, ensuring that the most valuable data are collected early while still retaining the flexibility to respond adaptively during construction. This synergy enhances risk management and supports more robust, cost-effective, and environmentally responsible decision-making in uncertain geological settings.

5.2.5 Single grouting design in each alternative

In this study, a single, fixed grouting design was adopted for each alternative, diverging from the observational method, which typically allows for adaptive design adjustments based on field observations. This simplification was made to enable a clear comparison of the overall impact of each grouting strategy across the entire tunnel and to assess the corresponding inflow levels for each alternative. Although this approach does not account for localized design optimization, it provides valuable insight into how each

predefined grouting scheme performs on a broader scale. Additionally, the analysis highlights the potential consequences of changes in failure criteria, such as revised inflow thresholds, and can serve as a tool to help designers anticipate the effects of modifying grouting strategies or performance requirements in future.

5.3 Future research

Given the inherent complexity and uncertainty in subsurface hydrogeological systems, ongoing research and methodological improvements remain essential. While this study provides a foundational framework for incorporating parameter uncertainty and evaluating the value of additional investigations, several assumptions and simplifications were necessary due to practical limitations such as time, data availability, and computational constraints. As tunnel projects become increasingly ambitious in scale and sensitivity, future studies can build upon the findings of this thesis by adopting more advanced models, integrating real-time monitoring data, and exploring alternative decision-support strategies. The following areas are identified as promising directions for further development:

5.3.1 Hydrogeological Model

5.3.1.1 Spatial Heterogeneity

Given the highly heterogeneous and anisotropic nature of fractured rock environments, incorporating spatially distributed hydraulic conductivity fields would likely enhance the realism of groundwater flow simulations. Approaches such as geostatistical modeling, conditional simulations, or stochastic realizations could be employed in future studies to better capture localized behavior and improve the reliability of tunnel inflow predictions.

5.3.1.2 Fracture orientation

Future research should prioritize incorporating detailed fracture orientation data into the hydrogeological modeling process. The current study did not explicitly account for directional properties such as dip, which are crucial in understanding preferential groundwater flow paths.

5.3.1.3 Grouting performance

Numerous factors influence the effectiveness of grouting, including the complex and irregular nature of actual fracture networks, which are often oversimplified in models. Additionally, variables such as the number and layout of grout holes in each fan, the injection pressure, grout mix properties, and the interaction between the grout and host rock all play significant roles. Therefore, future studies should focus on integrating more realistic geological conditions, use of Rock Classification System such as Rock Quality Designation (RQD), Rock Mass Rating (RMR), and the Rock Tunneling Quality Index (Q - method) to assess rock and detailed grouting parameters to better understand and predict the changes in hydraulic conductivity following grouting.

5.3.1.4 Transient model

This study is based on a steady-state model, which restricts the analysis by assuming constant hydraulic boundary conditions, such as recharge rates, and neglects the stor-

age properties of the aquifer. However, these factors can significantly influence the accuracy of model predictions, particularly under variable conditions. Therefore, future research should incorporate transient simulations to better capture the dynamic nature of groundwater systems and provide a more realistic representation of natural processes.

Incorporating time-dependent variations would allow for assessment of seasonal fluctuations, delayed responses to infiltration, and long-term trends due to climate change or anthropogenic influences. This would enhance the model's reliability for infrastructure planning and groundwater management under changing environmental conditions.

5.3.1.5 Probability distribution

This study was restricted to using a single triangular distribution for each fracture category. These distributions were applied to represent the epistemic uncertainty, i.e., the lack of knowledge regarding the representative hydraulic conductivity of entire fracture or weakness zones, rather than natural spatial variability within them. Future research should examine model sensitivity when the bounds of the triangular distribution are adjusted, as this would reflect the effect of incorporating new data and updating the distribution. In general, as more data becomes available, the spread or variation in the distribution is likely to narrow.

5.3.1.6 Use of parameter estimation PEST

Parameter estimation using PEST could support calibration and uncertainty analysis, particularly for hydraulic conductivity. While not fully applied in this thesis, it holds potential for future refinement. PEST enables the inverse calibration of multiple plausible model parameter sets, each consistent with observed data but representing the uncertainty in subsurface conditions. A similar approach was adopted by Sundell et al. (2019) for economic valuation of hydrogeological information.

5.3.1.7 Monte carlo simulation

A promising avenue for future research involves applying Monte Carlo simulation to enhance the probabilistic analysis of hydrogeological and grouting performance. In this study, a limited number of realizations were used to explore the impact of hydraulic conductivity uncertainty. However, Monte Carlo methods offer a more robust and statistically sound approach by allowing thousands of randomized realizations based on defined probability distributions of different input parameters. This would provide more detailed insight into the variability of model outputs, such as tunnel inflow rates and failure probabilities, and strengthen the statistical confidence in VOIA results.

In addition to providing a probabilistic spread of outcomes, Monte Carlo simulation enables global sensitivity analysis, which can identify the most influential parameters in the model. Understanding which input parameters, such as hydraulic conductivity, grouted conductivity, recharge or detection probabilities, drive the largest changes in model outputs can prioritize data collection efforts and optimize investigation strategies. This is particularly relevant in the context of Value of Information Analysis (VOIA), where targeted reduction of uncertainty in the most sensitive parameters can yield the highest return on investment.

5.3.1.8 Improving computational efficiency

As previously discussed, the limitation associated with GUI could be substantially improved by transitioning to FloPy, a Python-based interface for MODFLOW. While this approach requires in-depth knowledge of FloPy as well as sufficient time and computational resources, it would allow for the automation of model runs using for-loops or similar scripting methods. Inputs could be updated programmatically for each iteration, and results could be extracted and stored automatically in a desired format. Such automation would eliminate the need for manual adjustments and data extraction, thereby saving substantial time and effort and enhancing the reproducibility of the analysis. Beyond relying solely on script-based approaches, other advanced tools or platforms could also be explored and utilized to enhance efficiency and flexibility in the modeling workflow.

The potential for integrating hydrogeological modeling with Bayesian updating techniques should also be explored. By combining predictive simulations with probabilistic updating based on new observations, future studies could improve the reliability of decision-making under uncertainty. This integrated approach allows models to evolve dynamically as new data becomes available, supporting more adaptive and informed design strategies.

5.3.2 VOIA

5.3.2.1 Expert judgement and bayesian updating

In this study, fixed conditional probabilities (e.g., $P(D|F) = 0.80$) were assumed to represent the reliability of the hydrogeological investigation methods, serving as a basis for Bayesian updating. However, these values were not derived from expert input, which introduces a level of subjectivity and simplification.

Incorporating expert judgment can enhance the robustness of such assumptions, especially when empirical data is scarce or when the performance of field methods under complex geological conditions is uncertain. Experts with experience in grouting performance, fracture characterization, and tunnel hydraulics could provide probabilistic estimates for:

- $P(D|F)$: Probability of detecting failure if failure exists.
- $P(D|\neg F)$: Probability of a false positive.
- $P(\neg D|F)$: Probability of missing a failure.
- $P(\neg D|\neg F)$: Probability of correctly identifying no failure.

These estimates could be elicited through structured interviews or formal expert elicitation techniques such as the Delphi method or probability encoding. Integrating expert-informed probabilities into the Bayesian framework would allow for more realistic updating of failure likelihoods and improve the credibility of the Value of Information Analysis (VOIA).

Such an approach would also support sensitivity analysis by quantifying the impact of uncertainty in expert estimates on the final decision-making outcome. While not implemented in the current study, expert judgment offers a valuable path for refining the assessment of investigative reliability in future VOIA applications.

5.3.2.2 Expanding grouting alternatives and VOIA for multi-option decision making

This study evaluated two specific pre-excavation grouting alternatives: Alternative A1 with 20 boreholes using cement grout, and Alternative A2 with 30 boreholes including silica sol in selected locations. However, in practical tunnel engineering, a wider range of grouting configurations could be explored by varying design parameters such as the number of boreholes per fan, fan length, grout material combinations, injection pressure, or sequencing strategies. Future studies could assess intermediate alternatives or adaptive designs that optimize the extent of grouting based on geological conditions observed in real-time.

Furthermore, extending the VOIA framework to accommodate more than two decision alternatives can significantly enhance its practical utility. In real-world applications, decision-makers often face a spectrum of grouting strategies rather than binary choices. Implementing a multi-alternative VOIA would enable ranking of all available options based on their expected net benefit under uncertainty, rather than selecting between only two predefined cases.

This multi-criteria decision framework could also account for additional objectives, such as environmental risk, construction time, or material sustainability, resulting in a more balanced and realistic appraisal of grouting strategies. However, expanding the number of alternatives would also increase the computational burden, especially when combined with probabilistic modeling. This would require a more automated simulation and analysis pipeline, potentially using tools like FloPy or model calibration frameworks such as PEST, to efficiently evaluate each alternative and its expected benefit from additional information.

5.3.2.3 Cost modeling improvements

In this study, the cost of failure was defined primarily as the expense of post-excavation grouting required to meet the specified inflow thresholds, following a simplified and conservative assumption based on earlier work by Zetterlund et al. (2011). While this provides a practical and measurable estimate, it does not capture the full economic impact of tunnel inflow-related risks.

Future work could explore more comprehensive cost modeling by incorporating additional failure cost components. These may include:

- Construction delays: Excessive groundwater inflow may halt or slow down excavation and grouting operations, leading to significant schedule overruns. Delay costs can be substantial, especially in large infrastructure projects with tight timelines.
- Contractual penalties and fines: Regulatory frameworks or construction contracts often define strict inflow limits and performance obligations. Exceeding these limits could result in financial penalties or loss of contractual bonuses.
- Environmental impact costs: In sensitive areas, such as near Lake Skiren, excessive drawdown or leakage could harm ecosystems. Although more complex to quantify, such externalities might be modeled as risk costs in future VOIA frameworks.
- Increased operation and maintenance (O&M) costs: Poor initial sealing could

result in long-term drainage requirements or water handling systems that add operational costs over the tunnel's life cycle.

Integrating these broader definitions of failure cost into the cost-benefit analysis (CBA) would improve the realism of the economic modeling and make the VOIA results more robust for real-world decision-making. Doing so would also enhance the ability to justify additional investigations or improved design measures based on a more complete understanding of economic risk.

6 Conclusion

This thesis demonstrates the applicability and relevance of the Value of Information Analysis (VOIA) framework in the context of tunnel design under hydrogeological uncertainty. The study focused on the *Kolmårdentunneln* project, where reducing groundwater inflow through effective grouting is essential. Two grouting alternatives were compared using probabilistic modeling, hydraulic testing, and economic evaluation through cost-benefit analysis.

The results indicate that enhanced grouting strategies, such as Alternative A2, which includes silica grout and additional boreholes, provide notably better control of groundwater inflow. The Value of Information Analysis (VOIA) proved effective in quantifying the benefit of acquiring additional data, even though the preferred decision remained unchanged in this case. However, had the scenario been different, where prior and pre-posterior analyses led to different optimal alternatives, the VOIA would have demonstrated its full potential by justifying targeted investments in further site investigations.

The probabilistic treatment of fracture hydraulic conductivity using triangular distributions helped capture uncertainty; however, the model was limited by assumptions such as homogeneous fracture properties and constant grouting effectiveness. Incorporating spatial variability, real-time monitoring, and adaptive design strategies (e.g., via the observational method) could enhance future analyses.

Furthermore, while the model simplified grouting effects by assigning fixed post-treatment hydraulic conductivities, actual performance depends on fracture aperture, grout type, pressure, and penetration, all of which should be integrated into future work. Similarly, the failure cost was estimated based on post-grouting requirements but could be expanded to include fines, delays, or reputational risks.

Overall, this study shows that integrating VOIA into early tunnel design decisions provides a structured, quantitative method for balancing investigation cost with uncertainty reduction. Although simplified, particularly in the estimation of several input parameters, the study nonetheless serves as an illustrative example of how to perform a VOIA, demonstrating all the necessary steps of the analysis. With further development and interdisciplinary collaboration, this approach could support more resilient, cost-effective, and environmentally responsible tunnel construction in complex geological settings.

7 References

Bedford, T., & Cooke, R. (2001). *Probabilistic risk analysis: Foundations and methods*. Cambridge University Press.

Chen, Y.-F., Hu, S.-H., Hu, R., & Zhou, C.-B. (2015). Estimating hydraulic conductivity of fractured rocks from high-pressure packer tests with an izbash's law-based empirical model. *Water Resources Research*, *51*(4), 2096–2118. https://doi.org/https://doi.org/10.1002/2014WR016458

Clyde, M., Cetinkaya-Rundel, M., Rundel, C., Banks, D., Chai, C., & Huang, L. (2022). *An introduction to bayesian thinking- a companion to the statistics with r course* (1st, Vol. 1). Coursera.

Davis, J. C. (2002). *Statistics and data analysis in geology* (3rd). Wiley.

Freeze, R. A., James, B., Massmann, J., Sperling, T., & Smith, L. (1992). Hydrogeological decision analysis: 4. the concept of data worth and its use in the development of site investigation strategies. *Groundwater*, *30*(4), 574–588. https://doi.org/10.1111/j.1745-6584.1992.tb01534.x

Freeze, R. A., Massmann, J., Smith, L., Sperling, T., & James, B. (1990). Hydrogeological decision analysis: 1. a framework. *Groundwater*, *28*(5), 738–766.

Grøv, E., & Woldmo, O. (2012). Modern pre-grouting technology in norway. In *Grouting and deep mixing 2012: Proceedings of the fourth international conference on grouting and deep mixing* (pp. 805–815). American Society of Civil Engineers (ASCE). https://doi.org/10.1061/9780784412350.0064

Gustafson, G., Claesson, J., & Fransson, Å. (2013). Steering parameters for rock grouting. *Journal of Applied Mathematics*, *2013*. https://doi.org/10.1155/2013/269594

Gustafson, G., Fransson, Å., Funehag, J., & Axelsson, M. (2004). Ett nytt angreppssätt för bergbeskrivning och analysprocess för injektering. *Väg- och vattenbyggare*, *4*.

Gustafson, G., & Stille, H. (2005). Stop criteria for cement grouting. *Felsbau*, *23*(3), 62–68.

Gustafson, G., & Walke, L. (2012). *Hydrogeology for rock engineers*. BeFo Stockholm.

Hernqvist, L., Butrón, C., Fransson, Å., Gustafson, G., & Funehag, J. (2012). A hard rock tunnel case study: Characterization of the water-bearing fracture system for tunnel grouting. *Tunnelling and Underground Space Technology*, *30*, 132–144. https://doi.org/10.1016/j.tust.2012.02.014

Hernqvist, L. (2009). *Characterization of the fracture system in hard rock for tunnel grouting* [PhD thesis]. Chalmers University of Technology.

Hughes, J. D., Langevin, C. D., & Banta, E. R. (2017). *Documentation for the modflow 6 framework* (tech. rep.). US Geological Survey.

Kissell, R., & Poserina, J. (2017). Chapter 4 - advanced math and statistics. In R. Kissell & J. Poserina (Eds.), *Optimal sports math, statistics, and fantasy* (pp. 103–135). Academic Press. https://doi.org/https://doi.org/10.1016/B978-0-12-805163-4.00004-9

Lindblom, U. (2010). *Bergbyggnad* (1st). Liber AB.

Merisalu, J., Rosé, L., Boström, M., & Welleman, A. (2020). Conditional design for groundwater drainage in underground construction. https://www.diva

-portal.org/smash/record.jsf?pid=diva2%3A1747467&dswid=8718

Merisalu, J., Sundell, J., & Rosén, L. (2021). A framework for risk-based cost–benefit analysis for decision support on hydrogeological risks in underground construction. *Geosciences*, *11*(2), 82. https://doi.org/10.3390/geosciences11020082

Moges, E., Demissie, Y., Larsen, L., & Yassin, F. (2021). Sources of hydrological model uncertainties and advances in their analysis. *Water*, *13*(1), 28.

Murphy, C. (1999). A model for optimizing the assembly and disassembly of electronic systems. *Electronics Packaging Manufacturing, IEEE Transactions on*, *22*, 105–117. https://doi.org/10.1109/6104.778170

Panday, S., Langevin, C. D., Niswonger, R. G., Ibaraki, M., & Hughes, J. D. (2013). *Modflow–usg version 1: An unstructured grid version of modflow for simulating groundwater flow and tightly coupled processes using a control volume finite-difference formulation* (tech. rep.). US Geological Survey.

Peck, R. B. (1969). Advantages and limitations of the observational method in applied soil mechanics. *Géotechnique*, *19*(2), 171–187. https://doi.org/10.1680/geot.1969.19.2.171

Sikdar, P. K. (2019). Pumping test for aquifers: Analysis and evaluation. In P. K. Sikdar (Ed.), *Groundwater development and management: Issues and challenges in south asia* (pp. 267–277). Springer International Publishing. https://doi.org/10.1007/978-3-319-75115-3_11

SIS. (2005). *Eurocode 7: Geotechnical design – part 1: General rules* [SS-EN 1997-1:2005]. Swedish Standards Institute.

Sundell, J., Norberg, T., Haaf, E., & Rosén, L. (2019). Economic valuation of hydrogeological information when managing groundwater drawdown. *Hydrogeol. J*, *27*, 1111–1130.

Sveriges geologiska undersökning. (2021a, September 2). *Kartvisaren berggrund 1:1 miljon*. Retrieved March 18, 2025, from https://apps.sgu.se/kartvisare/kartvisare-berggrund-1-miljon.html

Sveriges geologiska undersökning. (2021b, December 28). *Kartvisaren jordarter 1:25 000–1:100 000*. Retrieved August 3, 2025, from https://apps.sgu.se/kartvisare/kartvisare-jordarter-25-100.html

Sveriges geologiska undersökning. (2023, November 23). *Kartvisaren hydraulisk konduktivitet i berg*. Retrieved March 16, 2025, from https://apps.sgu.se/kartvisare/kartvisare-hydraulisk-konduktivitet.html

Sweco. (2021). *Injection concept stavsjö–loddby, ostlänken* (Technical Report). Sweco.

Trafikverket. (n.d.). *Ostlänken – en ny dubbelspårig järnväg*. Retrieved February 21, 2025, from https://www.trafikverket.se/vara-projekt/projekt-som-stracker-sig-over-flera-lan/ostlanken-en-ny-dubbelsparig-jarnvag

Trafikverket. (2021). *Ostlänken – delen stavsjö-loddby: Tekniskt pm berg* (Technical Report). Trafikverket.

Trafikverket. (2022). *Ostlänken – delen stavsjö-loddby: Pm beräkningar. bilaga d2 till pm yt- och grundvatten* (Technical Report). Trafikverket.

Trafikverket. (2024). *Fastställelsehandling ostlänken, järnvägsplan delen stavsjö-loddby* (Technical Report). Trafikverket. https://bransch.trafikverket.se/contentassets/305ce34da86542caafe13244c06ba8ee/stavsjo

-loddby/faststallelse/planbeskrivning-jp-stavsjo-loddby-20240118.pdf

Winston, R. (2009). *Modelmuse-a graphical user interface for modflow-2005 and phast*.

Xia, Q., Xu, M., Zhang, H., Zhang, Q., & Xiao, X.-x. (2018). A dynamic modeling approach to simulate groundwater discharges into a tunnel from typical heterogenous geological media during continuing excavation. *KSCE Journal of Civil Engineering*, *22*, 341–350. https://doi.org/10.1007/s12205-017-0668-9

Zetterlund, M., Norberg, T., Ericsson, L. O., & Rosén, L. (2011). Framework for value of information analysis in rock mass characterization for grouting purposes. *Journal of Construction Engineering and Management*, *137*(7), 486–497. https://doi.org/10.1061/(ASCE)CO.1943-7862.0000265

Zetterlund, M. S., Norberg, T., Ericsson, L. O., Norrman, J., & Rosén, L. (2015). Value of information analysis in rock engineering: A case study of a tunnel project in Äspö hard rock laboratory. *Georisk: Assessment and Management of Risk for Engineered Systems and Geohazards*, *9*(1), 9–24. https://doi.org/10.1080/17499518.2014.1001401

Zurbuchen, B., Zlotnik, V., & Butler Jr, J. (2002). Dynamic interpretation of slug test in highly permeable aquifers. *Water Resources Research - WATER RESOUR RES*, *38*. https://doi.org/10.1029/2001WR000354

Appendix A

The following figures show the deformation zone in the study area.

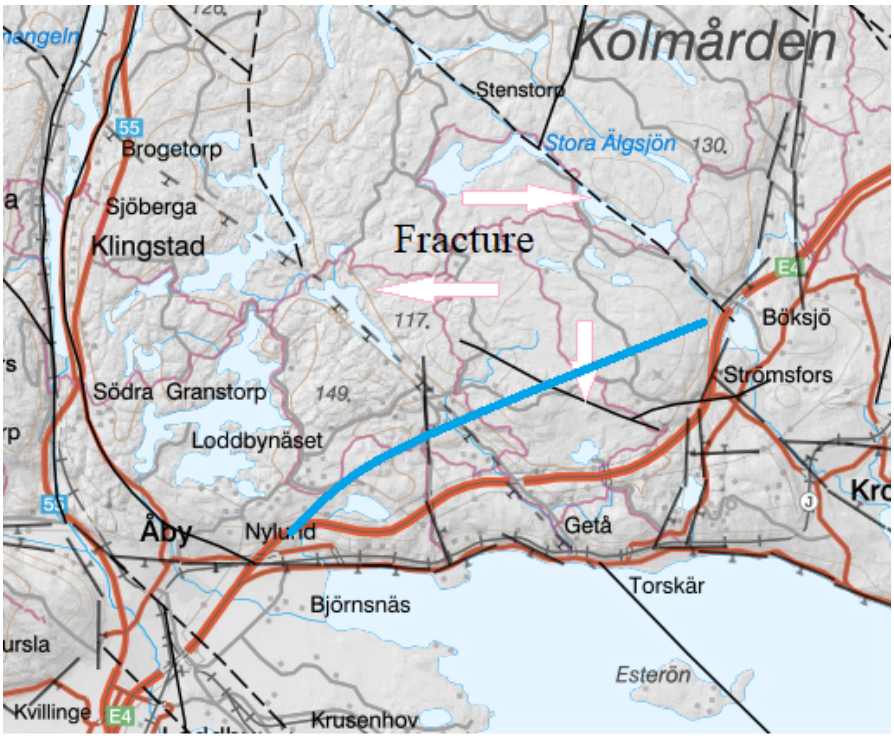

Figure A.1: The deformation zone interpreted by SGU in Kolmården is depicted, the blue line represents the tunnel geometry.

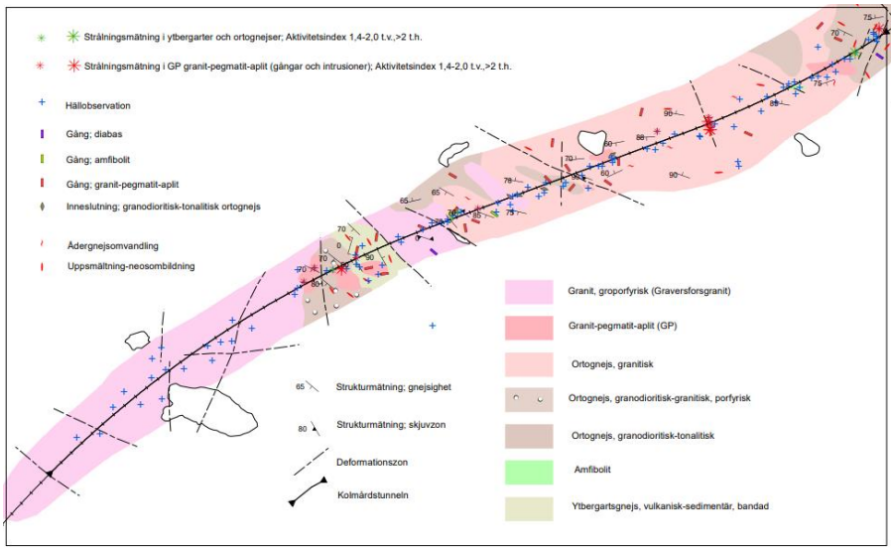

Figure A.2: The deformation zone along the tunnel as interpreted by SGU. Figure after Trafikverket, 2021

Appandix B

The following tables presents the results from various hydraulic tests, including the falling head method, pumping tests, and water loss measurements.

Table B.1: Hydraulic Test (Falling Head Method) Results in Stavsjö-Loddby Section

Serial Number	ID	K (m/s)
1	15S302GU	3,7E-07
2	15S303GU	2,9E-06
3	15S305GU	3,5E-06
4	15S306GU	2,1E-04
5	15S309GU	7,7E-06
6	15S310GU	3,2E-05
7	15S311GU	1,6E-05
8	15S312GU	2,9E-03
9	15S313GU	3,1E-05
10	15S314GU	1,4E-04
11	16S316GU	
12	16S317GU	
13	16S318GW	
14	16S319GU	
15	16S319GU	
16	16S319GU	
17	16S320GU	3,2E-07
18	16S321GU	1,2E-04
19	16S322GU	1,2E-04
20	16S323GU	
21	16S324GU	8,0E-06
22	16S325GU	1,6E-05
23	16S326GU	6,8E-05
24	16S327GU	7,0E-07
25	16S330GU	4,9E-07
26	16S331GU	2,6E-07
27	16S333GU	
28	16S334GU	2,0E-05
29	16S335GU	3,3E-04
30	16S336GU	
31	16S337GU	4,9E-05
32	16S338GU	
33	16S339GU	8,4E-06
34	16S340GU	6,2E-05
35	16S341GU	2,0E-07
36	16S342GU	2,6E-06
37	16S343GU	4,3E-06
38	17S302GU	4,7E-05
39	17S303GU	7,8E-05
40	17S304GU	1,2E-05

Serial Number	ID	K (m/s)
41	17S306GU	2,3E-05
42	18S301GU	3,1E-05
43	18S301GW	1,1E-06
44	18S303GU	1,8E-05
45	18S304GU	6,4E-06
46	18S305GU	3,8E-08
47	18S306GU	5,5E-06
48	18S307GU	2,1E-07
49	18S308GU	3,6E-06
50	18S309GU	3,4E-07

Table B.2: Results from Pumping Test.

ID	Borehole Type	K [m/s]
17S122BR	139 mm well	5.5E-07

Table B.3: Compilation of results from water loss measurements. The values are geometric means. The table presents ID, total length of the hole, evaluated hydraulic conductivity (K) for full and half holes.

ID	Total Length [m]	K half-hole [m/s]	Section [m]	K full-hole [m/s]	Section [m]
15S1KB01	119.25	2.6E-07	61.5-119.4	2.8E-07	4.0-119.4
15S1KB02	110.15	2.0E-06	58.0-110.0	3.7E-06	6.0-110.0
16S1KB03	100.8	2.8E-07	50.0-105.0	4.5E-07	15.0-100.8
16S1KB04	47.3	*	-	4.2E-07	21.0-47.0
16S1KB05	67.1	*	-	*	-
16S1KB08	49.9	2.2E-08	25.0-49.9	6.3E-08	19.0-49.9
16S1KB09	49.4	8.8E-09	28.0-49.4	3.9E-08	7.0-49.4
16S1KB11	69.7	1.7E-08	35.0-69.7	2.3E-07	3.0-69.7
16S1KB12	32.1	5.8E-09	13.5-32.1	1.8E-07	20.0-32.1
16S1KB13	77.15	2.2E-07	33.0-77.0	3.1E-07	11.0-77.0
17S1KB15	92.9	2.8E-07	43.5-92.9	*	-
18S1KB17	101	1.5E-08	50.0-100.0	2.3E-06	7.0-100.0
BVKB01	45.8	*	-	*	-
BVKB02	53.4	1.1E-06	32.5-52.5	6.0E-06	13.5-52.5
17HB101	100	2.5E-07	5.0-100.0	4.5E-06	5.0-100.0
17HB102	100	8.2E-07	50.0-100.0	1.9E-06	5.0-100.0
17HB103	120	2.4E-09	60.0-120.0	4.5E-08	6.0-120.0
17HB104	100	7.8E-08	50.0-100.0	9.0E-08	11.5-100.0
17HB105	90	7.1E-09	45.0-90.0	9.5E-06	7.0-90.0
17HB106	50	8.8E-08	25.0-50.0	3.4E-07	5.0-50.0

Table B.4: Summary of bedrock conductivity evaluated from water loss measurement along the Stavsjö - Loddby section (from south to north along the alignment

Area	Chainage	Borehole ID	Conductivity [m/s]
Skiren	101+550	15S1KB02	$1{,}33 \cdot 10^{-7}$
Skiren	102+500	14S1KB03	$2{,}81 \cdot 10^{-7}$
Skiren	101+050	16S1KB04	$1{,}00 \cdot 10^{-8}$
Getå	98+850	16S1KB08	$2{,}21 \cdot 10^{-8}$
Böksjötorp	94+600	16S1KB09	$9{,}93 \cdot 10^{-9}$
Böksjötorp	94+300	16S1KB11	$2{,}92 \cdot 10^{-8}$
Getå	98+850	16S1KB12	$1{,}00 \cdot 10^{-8}$
Getå	99+450	16S1KB13	$2{,}23 \cdot 10^{-7}$
Getå	99+300	17S1KB15	$2{,}85 \cdot 10^{-7}$
Skiren	101+650	18S1KB17	$9{,}09 \cdot 10^{-10}$
Skiren	101+900	17HB101	$1{,}50 \cdot 10^{-8}$
Skiren	101+500	17HB102	$4{,}98 \cdot 10^{-8}$
Böksjötorp	98+000	17HB103	$2{,}38 \cdot 10^{-9}$
Böksjötorp	97+100	17HB104	$7{,}82 \cdot 10^{-8}$
Böksjötorp	96+300	17HB105	$7{,}06 \cdot 10^{-9}$
Böksjötorp	95+200	17HB106	$8{,}79 \cdot 10^{-8}$

Appendix C

Table C.1: Ground water well data with levels in RH2000.

ID	Pipe top edge	Ground level	Avg level	Max-level	Min-level
15S113GU	73.6	72.3	59.2	59.7	58.8
16S104GU	45.7	44.6	44.4	44.6	43.8
16S113GU	97.6	96.4	96.2	96.7	95.7
16S115GU	79.7	78.8	78.2	79.5	76.4
16S116GU	129.5	128.4	128.0	128.3	127.0
16S117GU	129.5	128.9	128.1	128.6	126.5
16S127GU	120.0	118.8	118.8	118.9	118.3
16S129GU	15.8	14.7	10.8	10.8	10.8
16S130GU	84.2	82.6	82.4	83.6	81.3
17S107GU	73.5	72.4	68.8	69.3	68.4
17S148GU	77.0	75.9	74.9	75.4	73.5
18S102GU	93.3	92.3	91.6	92.3	90.9
17S102GU	76.4	76.4	74.2	75.4	73.8
17S146GU	85.9	85.9	84.0	84.4	83.3
16S112GU	31.1	31.1	28.9	30.5	27.7
Graoundwater well in rock					
17HB101	–	102.7	101.4	–	–
17HB102	–	140.0	137.3	–	–
17HB103	–	138.7	136.0	–	–
17HB104	–	137.5	135.4	–	–
17HB105	–	118.2	117.5	–	–
17HB106	–	94.8	93.3	–	–
18S1KB17	–	84.7	81.3	–	–

Appandix D

The tables below display various realizations of fracture hydraulic conductivity, along with a representative example of output generated from ModelMuse and PEST. This includes a comparative assessment between observed and simulated hydraulic heads.

Table D.1: Sampled hydraulic conductivity values for General Fracture ($k_{general}$) and Getå Fracture ($k_{getå}$)

Sample No.	$k_{general}$ **(m/s)**	$k_{Getå}$ **(m/s)**
1	1.00×10^{-9}	1.00×10^{-9}
2	1.10×10^{-9}	1.81×10^{-9}
3	1.81×10^{-9}	7.47×10^{-9}
4	3.73×10^{-9}	2.28×10^{-8}
5	7.45×10^{-9}	5.27×10^{-8}
6	1.36×10^{-8}	1.02×10^{-7}
7	2.27×10^{-8}	1.75×10^{-7}
8	3.53×10^{-8}	2.75×10^{-7}
9	5.19×10^{-8}	4.08×10^{-7}
10	7.29×10^{-8}	5.77×10^{-7}
11	9.87×10^{-8}	7.83×10^{-7}
12	1.30×10^{-7}	1.03×10^{-6}
13	1.66×10^{-7}	1.32×10^{-6}
14	2.07×10^{-7}	1.65×10^{-6}
15	2.54×10^{-7}	2.02×10^{-6}
16	3.05×10^{-7}	2.44×10^{-6}
17	3.61×10^{-7}	2.88×10^{-6}
18	4.21×10^{-7}	3.36×10^{-6}
19	4.83×10^{-7}	3.86×10^{-6}
20	5.48×10^{-7}	4.38×10^{-6}
21	6.14×10^{-7}	4.91×10^{-6}
22	6.79×10^{-7}	5.43×10^{-6}
23	7.42×10^{-7}	5.94×10^{-6}
24	8.02×10^{-7}	6.42×10^{-6}
25	8.57×10^{-7}	6.85×10^{-6}
26	9.05×10^{-7}	7.24×10^{-6}
27	9.45×10^{-7}	7.56×10^{-6}
28	9.75×10^{-7}	7.80×10^{-6}
29	9.94×10^{-7}	7.95×10^{-6}
30	1.00×10^{-6}	8.00×10^{-6}

Table D.2: Comparison of Measured and Modeled Heads with Residuals for realization 1

Observation Name	Measured (m)	Modeled (m)	Residual (m)	Residual^2 (m^2)
_16S115GU	78.23	62.213	16.017	256.55
_17HB102	101.355	96.974	4.381	19.19
_16S104GU	44.39	40.784	3.606	13.01
_16S129GU	10.8	14.181	-3.381	11.42
_17S107GU	68.79	71.482	-2.692	7.25
_17HB103	137.33	135.132	2.198	4.83
_17S102GU	74.2	76.100	-1.900	3.61
_17HB104	136.019	134.233	1.786	3.19
_17HB101	81.305	82.744	-1.439	2.07
_16S113GU	96.18	97.305	-1.125	1.27
_16S127GU	118.81	119.678	-0.868	0.75
_17HB105	135.352	135.811	-0.459	0.21
_16S130GU	82.44	82.607	-0.167	0.03
			Sum of Squared Residuals	**323.38**

DEPARTMENT OF ARCHITECTURE AND
CIVIL ENGINEERING
CHALMERS UNIVERSITY OF TECHNOLOGY
Gothenburg, Sweden 2025
www.chalmers.se

CHALMERS
UNIVERSITY OF TECHNOLOGY